

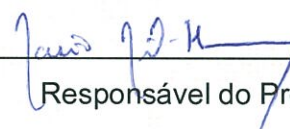
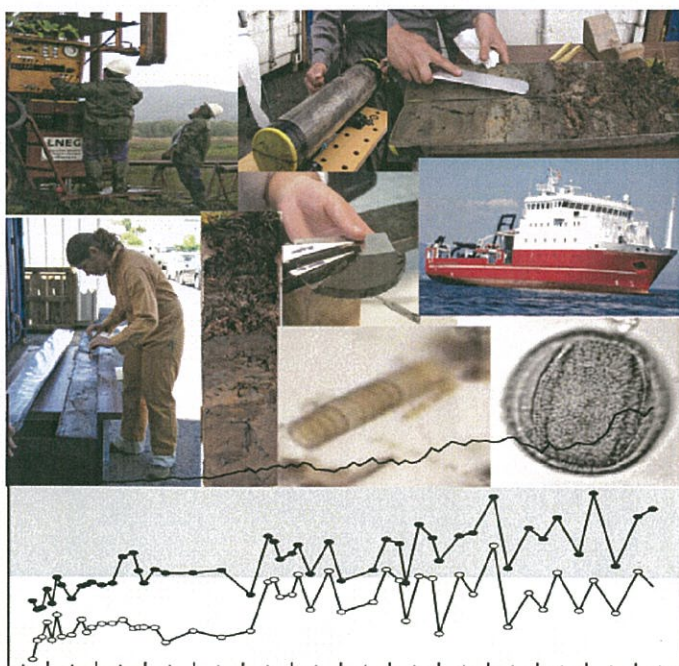
**Project NATURA MIÑO-MINHO “Valorización de los recursos de la
cuenca hidrográfica del MIÑO-MINHO”
Activity 1 report – Part 2**

**Characterization of DIVA09 – a gravity core from
the Minho shelf**

Mário Mil-Homens¹, Filipa Naughton¹, Ana M. Costa¹, Dulce Oliveira¹, Célia Santos¹,
Teresa Rodrigues¹, Fátima Abrantes¹
Sandra Fonseca², Raquel Serrano²

¹ CIIMAR / Unidade de Geologia Marinha - Laboratório Nacional de Energia e Geologia

² Núcleo Operacional de Química Inorgânica - Laboratório de Referência do Ambiente – Agência Portuguesa do Ambiente



Responsável do Projecto

Aprovado para distribuição

Data 01/06/2012



O Interlocutor da Unidade de Geologia
Marinha



Ministério de Economia e do Emprego

Laboratório Nacional de Energia e Geologia

Estrada da Portela – Zambujal

Apartado 7586

2610-999 AMADORA



PROGRAMA
COOPERACIÓN TRANSFRONTERIZA
ESPAÑA ~ PORTUGAL
COOPERAÇÃO TRANSFRONTEIRIÇA
2 0 0 7 – 2 0 1 3



União Europeia
FEDER

Investimos no seu futuro

Project NATURA MIÑO-MINHO “Valorización de los recursos de la cuenca hidrográfica del MIÑO-MINHO”

Activity 1 report – part 2

Characterization of DIVA09 – a gravity core from the Minho shelf

Mário Mil-Homens¹, Filipa Naughton¹, Ana M. Costa¹, Dulce Oliveira¹,
Célia Santos¹, Teresa Rodrigues¹, Fátima Abrantes¹
Sandra Fonseca², Raquel Serrano²

¹ CIIMAR / Unidade de Geologia Marinha - Laboratório Nacional de Energia e Geologia

² Núcleo Operacional de Química Inorgânica - Laboratório de Referência do Ambiente - Agência Portuguesa do Ambiente

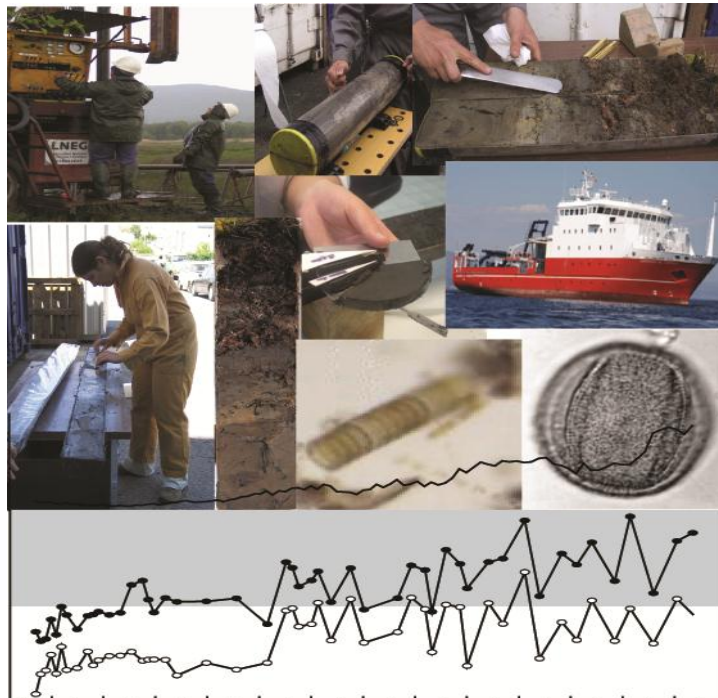


Table of Contents

Abstract	1
Introduction	1
Environmental setting	2
Materials and Methods	5
Mechanical drills.....	5
Brief mechanical cores description	5
Gravity core sampling	6
Brief gravity core description	6
Type of analysis	7
Carbon-14.....	7
Lead-210.....	7
Grain size.....	7
Foraminifera.....	8
Diatoms.....	8
Geochemistry.....	9
Biomarkers.....	11
Pollens.....	11
Results	12
Chronostratigraphy	12
Grain size.....	15
Foraminifera.....	17
Diatoms.....	18
Geochemistry.....	20
Organic carbon, total nitrogen and calcium carbonate.....	20
Major and trace elements.....	21
Biomarkers.....	27
Pollens.....	28
Discussion	31
Temporal variability in organic matter composition	31
Selection of the normalizer element.....	33
Temporal variability in supply of terrigenous materials	34
Climatic changes in the NW Portuguese Margin and the influence of human activities since the last 2500 years	36
Sub-orbital climate variability during the late Holocene.....	37
Summary and final considerations	42
Acknowledgments	43
References	43

Abstract

The overall objective of the Natura Miño-Minho project is to contribute for a better understanding of the Minho river ecosystem in order to assure a correct management and preservation of its natural resources. This report aims to describe the actions that took place within Activity 1 of the Natura Miño-Minho project. This activity was divided in two distinct parts; a first part involving the study of sediments as a tool for identifying possible areas specially marked by anthropogenic impacts (considering a spatial perspective) in the estuary and a second part focused on the use of sediments as a key for improving the knowledge associated with climatic variability and human activities (agriculture, (de)forestation, ...) through time. To reach this goal a set of mechanical drills were recovered from within the estuary. Additionally, a gravity core (DIVA09) was collected on the continental shelf, in the Galicia Mud Patch, to allow a comparison of the sedimentary records. A multi-parameter approach (pollen, diatoms, biomarkers, grain-size, organic carbon, determinations, stable oxygen isotopes, major and trace elements) was initially proposed to apply in both the estuarine and the marine cores, which were to be dated by ^{210}Pb and ^{14}C . Nevertheless, the difficulties in the establishment of geochronologies for the estuarine cores, due to the occurrence of sedimentary disturbances and the need for further analyses not possible for lack of funds, not allowed developing the temporal reconstruction of estuarine sedimentary sequences. Therefore, the temporal reconstruction is confined uniquely to the DIVA09 core. Anyway, the multi-parameter analyses performed down-core is indicative of an evolution of the hydrodynamic conditions (resulting from different oceanographic conditions induced both by global climate variability and small sea-level oscillations) and the resulting regional climate conditions through time as shown by Sea Surface Temperature gradually decreasing trend up to the present, but superimposed onto the orbitally induced long-term cooling pattern.

On the shelf, the multi-parameter analyses included pollen, SST and planktonic $\delta^{18}\text{O}$ and allowed the identification of sub-orbital climatic variability during the last 2500 years. Additionally, despite the influence of hydrodynamic conditions in the preservation of the sediment record, grain-size, pollen, n-alcohols and n-alkanes data suggest a gradual increase of continental input during the Roman Warm Period and the Dark Ages.

Introduction

NATURA MIÑO-MINHO project – “Valorización de los recursos de la cuenca hidrográfica del Miño-Minho” is a project developed between Portugal and Spain financed by European Union through the *Programa de Cooperação Transfronteiriça Espanha-Portugal* (POCTEP/FEDER) in order to get scientific knowledge related to environmental conditions existing in the Minho estuary and adjacent shelf area. The main goals of the project are evaluating climatic changes in the NW Portuguese Margin and the influence of human activities in local environments. Improvement of the knowledge's level will allow implementing management policies assuring preservation and integration of natural resources, promotion of sustainable development and biodiversity conservation of the Natura 2000 network habitats. The work developed in Activity 1 was only possible due to the intense and profit collaboration with other research groups (Núcleo Operacional de Química Inorgânica - Laboratório de Referência do Ambiente – Agência Portuguesa do Ambiente; Unidade de Sondagens; Laboratório Nacional de

Energia e Geologia; Universidad de Vigo; Royal Netherlands Institute for Sea Research - Department of Marine Geology) although not partners of this project.

Through the study of sedimentary sequences and sediment components it is possible to reconstruct environmental conditions existing on continents and oceans in the Past. Sediments constitute sensitive temporal indicators that are useful for reconstructing the history of sediment deposition (Valette-Silver, 1993) in terms of monitoring climatic evolution and recording evolution of anthropogenic impacts over time. This potential for “memorizing” the past environmental conditions makes sediments a powerful tool for predicting the environmental evolution of the planet Earth in the future.

In order to attempt characterizing past environmental changes of the Minho estuary a set of mechanical drills were collected in the Salcidos region and to comparing estuarine and shelf records, a sediment core collected on the adjacent shelf area was also studied. This part of the continental shelf is characterized as a favorable environmental setting for accumulation of fine-grained sediments, and consequently formation of fine-grained shelf depocenters identified in previous studies (Araújo et al., 2002; Dias et al., 2002a; Dias et al., 2002b; Lantzsch et al., 2009a; Lantzsch et al., 2009b; Lantzsch et al., 2010). One of these deposits, named Galicia Mud Patch (GMP) by Dias et al. (2002a), is characterized by a North-South orientation and formed in water depths around 100-120m. With the main objective of reconstructing environmental conditions existing in this area in the recent past, ^{210}Pb and ^{14}C determinations were used as a basis for age model definition. Furthermore, a set of inorganic and organic sediment components (diatoms, pollens, biomarkers, organic carbon, grain size, major and trace element concentrations) were studied on both sedimentary sequences.

Environmental setting

The NW Iberian Continental shelf is relatively narrow, ranging between 30 and 50km of extension (Figure 1; e.g. Dias et al., 2002a). The inner shelf is characterized by the occurrence of plutonic and metamorphic outcrops; while outer shelf outcrops are formed by Mesozoic and Cenozoic rocks (Dias et al., 2002a). Outcrops create sheltered environments with different deposition conditions leading to the accumulation of fine and well sorted sands in the inner shelf (<30km), coarse sands and gravel in the mid-shelf and medium sands between Mesozoic and Cenozoic crops (van Weering et al., 2002). The shelf break generally occurs at water depths of 160 to 180m (Dias et al., 2002a). The slope is steep and irregular plunging to the abyssal plain.

In the NW Iberia, five rivers (Douro, Ave, Cávado, Lima and Minho) are the main sediment suppliers to the adjacent continental margin. The Douro river is the main sediment supplier (ca.

8.2x10⁹m³ annual discharge) corresponding to ca. 87% of all fluvial sediments in the area (Dias, 1987), followed by the Minho river (e.g. Dias et al., 2002b; Jouanneau et al., 2002; Oliveira et al., 2002b). The Douro River have 927km length, draining a catchment area of 97682km² (Loureiro et al., 1986), mainly formed by granitic rocks and metamorphic rocks of Palaeozoic age (schists, gneisses, micaschists and greywackes) (Oliveira et al., 2002a). The Minho River is located in the western Iberian margin, in the border region between Minho (Portugal) and Galicia (Spain), and discharges to the Atlantic Ocean with a mean annual freshwater discharge of 300m³s⁻¹. It is 300km long and has a 17081km² watershed that extends mostly over Galicia, Spain, with less than 5% of its area in Northern Portugal (Loureiro et al., 1986). The last 70km of the Minho River form the natural border between Portugal and Spain, which includes the main estuarine axis of approximately 40km corresponding to the area under the influence of the spring tides (Sousa et al., 2005). The Minho is classified as a mesotidal estuary with a tidal range varying from about 2m at neap tides to about 4m at spring tides (Bettencourt and Ramos, 2003). The sediments of Minho River are essentially composed by sand (median contents of 80%) with the predominance of coarse sands (see grain-size data included in Activity 1 report part 1). The river basin occupies an area dominated by rock formations of the pre-Ordovician Schist-greywacke Complex and granites.

The sedimentation on the NW Iberian margin is complex and essentially sustained by episodic flood events (Dias et al., 2002b) and/or during maximal episodes of river outflow (Araújo et al., 1994; Drago et al., 1998). Fine-grained sediments, after being released by rivers mainly during the winter seasons, are transported in nepheloid layers (Bottom – BNL, intermediate – INL and surface – SNL) to the outer shelf. High hydrodynamic conditions during extreme storm events (downwelling conditions), induce re-suspension of fine-grained fluvio-genic sediments during winter and transport to north by poleward-flowing current (Drago et al., 1998; Dias et al., 2002b; Jouanneau et al., 2002; van Weering et al., 2002). The availability of fine-sediments, morphological barriers and hydrological conditions leads to the formation of mud depocenters (Dias et al., 2002b) at around 100-120 meters water depth (mwd), listed from south to north as: Douro Mud Patch, Galicia Mud Patch and Muros Mud Patch. During upwelling conditions, fine sediment export is restricted to the shelf edge (McCave and Hall, 2002; van Weering et al., 2002).

The present-day climate and vegetation in the NW part of Spain, including the Minho basin, is influenced by wet, relatively cool and weakly seasonal Atlantic climate (annual precipitation mean: 900-1400mm yr⁻¹ and temperature range: -7 to 10°C) and is dominated by deciduous *Quercus* forest (*Q. robur*, *Q. pyrenaica* and *Q. petraea*), heath communities (Ericaceae and *Calluna*) and *Ulex*. There are also locally birch (*Betula pubescens* subsp. *celtibérica*) and hazel (*Corylus avellana*) groves, and

brooms (*Genista*) (Alcara Ariza et al., 1987). The Douro River hydrographic basin is characterized by high precipitation values (700 to 1000mm yr⁻¹) and winter temperatures between -4 and 4°C. At high altitudes, the wettest and coldest zones reach 1600mm yr⁻¹ and -8°C, respectively (Polunin and Walters, 1985). The oceanic influence is particularly important in the northwest of the basin, where the *Q. robur* and *Q. suber* association predominates (Braun-Blanquet et al., 1956). The spread of both *Pinus pinaster* and *Eucalyptus globulus* has been favored by anthropic impact. The understory vegetation is largely dominated by *Ulex*, in association with heaths. The river margins are colonized by *Alnus glutinosa*, *Fraxinus angustifolia*, *Ulmus* spp., *Salix* spp., and *Populus* spp..

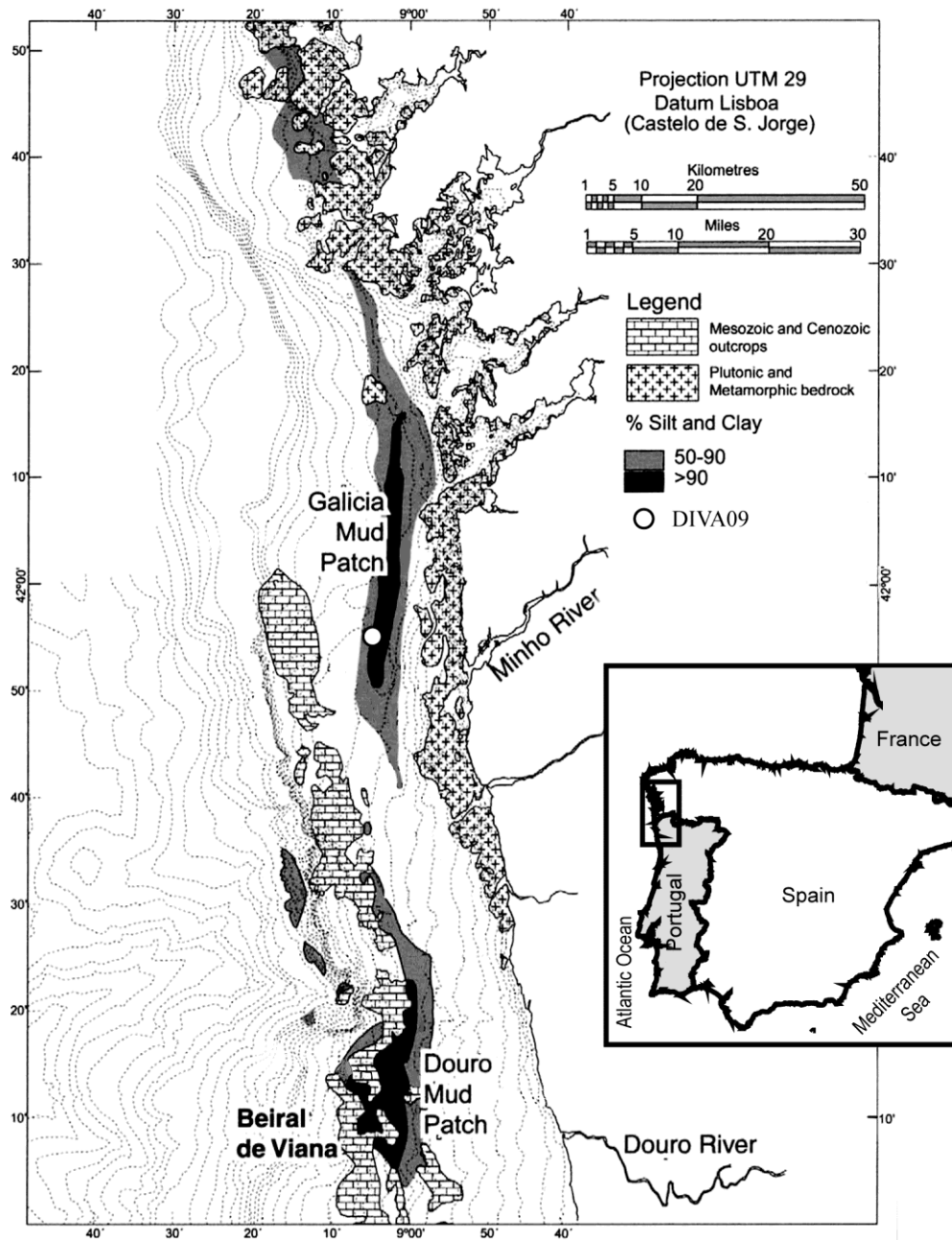


Figure 1 – Map of the study area and location of DIVA09 adapted from Dias et al., (2002a).

Materials and Methods

Mechanical drills

A set of 7 mechanical drills were collected in the Minho estuary, La Guardia area, with the aim of recovering the thick muddy Pleisto-Holocene sediments. These cores were recovered on April 2010 (Figure 2) with a Bonne Esperance FBEZN corer mounted on a 6x4 truck. In the laboratory all cores were opened, described and photographed prior to being stored at 4°C.

Brief mechanical cores description

From the 7 mechanical cores only 3 were considered as not mixed with falling surface sediments and representing a good sequence of estuarine sediments:

- MS02 – composed by 8 sections, with a total length of approximately 820cm including all sections and core catchers and representing a drill of 943cm;
- MS05 – composed by 8 sections, with a total length of approximately 1130cm including all sections and core catchers and representing a drill of 928cm;
- MS06 – composed by 7 sections, with a total length of approximately 860cm including all sections and core catchers and representing a drill of 957cm.

These 3 mechanical cores were recovered at the same place (Figure 2) and are composed by silt/clay sediment coarsening with depth to coarse sand and pebbles at core bottom. At the top centimeters all cores show a well-developed soil with ca. 12cm, followed by shingles (especially bricks) from an old road until ca. 30cm. At certain core depth (210cm to MS06, 284cm to MS05 and 255cm to MS02) shell fragments appear until the core bottom. Pebbles occur at ca. 750cm in MS06 and MS02, while in MS05 the contact to the pebbles layer is at the core bottom. Almost all sections showed at the top centimeters a layer of mixed sediment that results from the recovery process, but the beginning of the next section was assigned at the point where the characteristics of the sediment became homogeneous. In order to attempt solving difficulties arose in the sequencing of the estuarine sections, the cores were analyzed by X-ray fluorescence (XRF) core-scanner. Nevertheless, the XRF results were not conclusive for the distinction between in loco and mixed parts. An attempt to do X-ray core imaging in a private company was done but the lack of funds at the time prevented us to go ahead with that analyses. Left with no clear chronologies, the group decided to leave the evaluation of the results for a later time when an age model can be established for the Minho Estuary cores.

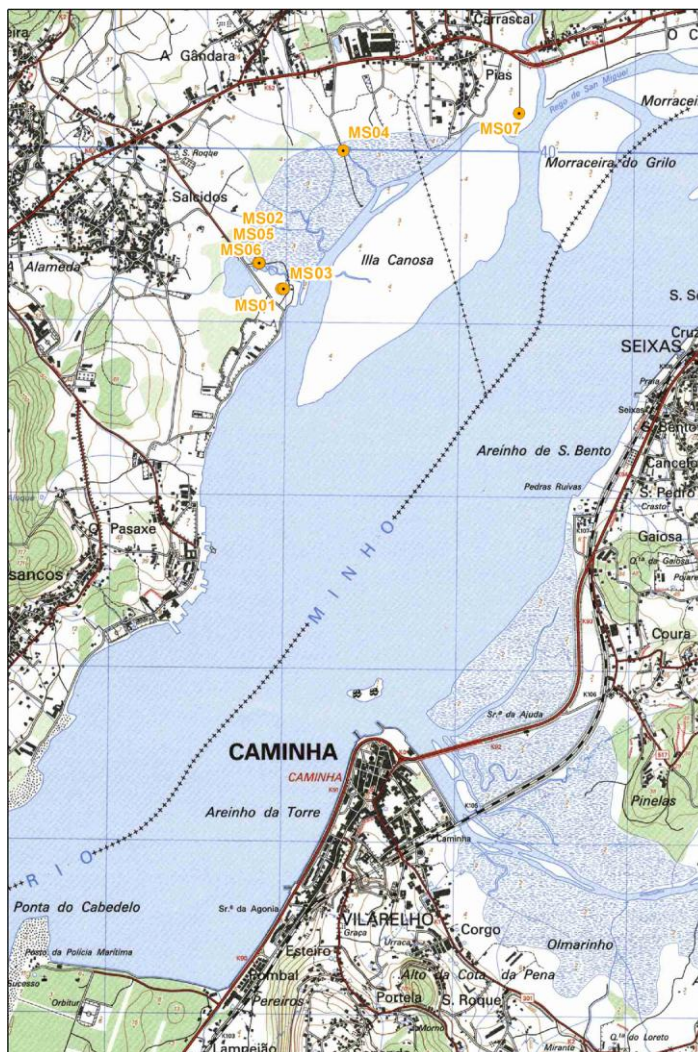


Figure 2 – Map showing the mechanical drill points (sheet 14 of the topographical map IGeoE).

Gravity core sampling

The gravity core used in the study, DIVA09 GC MMH1 (for now on referred as DIVA09), was recovered by Vigo University with the R.V. Sarmiento de Gamboa in October 2009 at 41°55.0105' N and 9°4.4108' W and 120 mwd (Figure 1) within the GMP. DIVA09 core was split and described. Shells and snails were collected for accelerator mass spectrometry AMS ¹⁴C. Half of the core was used for XRF core-scanner measurements and stored at 4°C for reference. After description, the other half-core was sub-sectioned in 1cm intervals. Each slice was split and stored for different analysis (10 cc for foraminiferal assemblages and texture, 4 cc for biomarkers, geochemistry and chronology; 4 cc for pollens; 2cc for diatoms).

Brief gravity core description

DIVA09 is 106 cm long, shows slight color variations with depth from (5Y 5/2) between 5 to 85cm to (5Y 4/2) below this depth. Part of the core top was lost (unknown extension of the lost

material). Sampling started at 4cm below existing top. Four shell fragments found along the core were collected for ^{14}C measurements.

Type of analysis

Carbon-14

Four marine carbonate samples collected at different depths (Table 1), were dated based on AMS radiocarbon measurements at the Leibniz-Laboratory for Radiometric Dating and Stable Isotope Research, Kiel, Germany.

Table 1 – Samples used for ^{14}C measurements and quantity of carbon in mg

Lab number	Sample name	Sample description	Amount of C analyzed (mg)
KIA 42919	DIVA09 3-4 cm	Snail	1.4
KIA 42920	DIVA09 57-58 cm	Shell	1.2
KIA 42921	DIVA09 83-84 cm	Shell	1.3
KIA 42923	DIVA09 101-102 cm	Shell	1.1

Lead-210

The activity of the isotope ^{210}Pb (with a half-life of 22.3 years) was measured with α -spectrometry using the grand-daughter isotope ^{210}Po , with a half-life of 138.4 days (e.g. Boer et al., 2006). These measurements were carried at the Department of Marine Geology - Royal Netherlands Institute for Sea Research, according to an in house methodology.

Grain size

Samples for grain-size measurements were prepared and analyzed according to the in-house method of Laboratório de Sedimentologia e Micropaleontologia da Unidade de Geologia Marinha - Laboratório Nacional de Energia e Geologia (UGM – LNEG), using a Sedigraph 7100 analyzer. This equipment is capable of measuring grain-sizes in the range of 0.01-63 μm . Briefly; samples were weighted and wet sieved through a 63 μm sieve. After dried, the fraction over 63 μm was weighted, and determined the corresponding percentage of sand in the total sample. The fraction above 63 μm was used for the determination of planktonic and benthic foraminifera species. The fraction below 63 μm was pre-treated organic matter destruction in order to obtain silt and clay % content. In a first step, 1ml of 0.033 M of sodium hexa-metaphosphate (Calgon) and 200ml of deionized water were added to the sample for 48 hours to disaggregate each sample. After this, different volumes (25 to 75ml per day, for at least 4 days) of hydrogen peroxide (H_2O_2) with ammonia ($\text{NH}_3\text{O} + \text{H}_2\text{O}_2$; 0.5ml of NH_3O per 100ml of H_2O_2) were added to remove all organic matter. The necessary volume of H_2O_2 depends on the quantity of organic matter contained in each sample. In order to remove the exceeding H_2O_2 released

during the previous chemical reaction, the solution was heated in a water bath at 60°C during 24 hours. For quickly eliminating the excess liquid, samples were washed approximately 6 times with 1000 ml of deionized water, using candle ceramic filters. Samples were poured in a glass flask with 1ml of Calgon to prevent flocculation and one drop of formaldehyde was added to avoid fungi development. Before analysis in the Sedigraph equipment, samples were homogenized with a vertical stirrer with 700 rpm for, at least, 15 minutes. In this work three grain-size classes were used, defined as:

- clay < 4µm;
- 4µm < silt < 63µm;
- 63µm < sand < 2000µm

The sample's classification into those three classes was determined through the use of the ternary diagram defined by (Shepard, 1954), with the support of the Visual Basic program developed by (Poppe and Eliason, 2008). This routine allows classifying sediments based on grain-size measurements. Clay and silt contents were measured with Sedigraph analyzer in the same samples used for geochemistry analysis.

Foraminifera

Oxygen isotopic compositions were determined on three planktonic foraminifera species: *Globigerina bulloides*, *Globigerina inflata*, and *Neobloquadrina pachyderma* (r) and the benthic genus *Uvigerina* sp.. The foraminifera shells (5-21 specimens) were collected from the sand fraction with a size larger than 150µm. Stable isotope ratios were analyzed on a Finnigan MAT 251 mass spectrometer at Marum, Bremen University (Germany). The $\delta^{18}\text{O}$ ratios are reported in per mil (‰) relative to the Vienna Peedee Belemnite standard (VPDB). Analytical standard deviation is $\pm 0.07\text{‰}$ for $\delta^{18}\text{O}$.

Diatoms

Siliceous microfossils analysis (diatoms and plant phytoliths) were carried out on surface samples, following the procedure of Abrantes et al. (2005). Sediment samples (2 – 2.5 g of bulk sediment) are placed in glass jars and are treated with Calgon in order to desegregate the clays. After this, alternate treatments with H₂O₂ and hydrochloric acid (HCl), at room temperature and over hot plates, were applied until all the organic matter and carbonate contents were removed. Distilled water is then used to wash the samples through siphoning in order to remove the clay content (this process is made with a minimum of 8 hour interval between siphoning). Calgon is then added as needed in order to release any extra clay content. Diatom slides are then prepared using sedimentation trays (Battarbee, 1973), and mounted with Permunt medium. Absolute abundance of diatoms valves (marine, brackish and freshwater) and phytolith cells are determined after slide quantification with x 1000 magnification,

using the counting protocol of Schrader & Gersonde (1978) and Abrantes (1988). Absolute abundance in any one level is based on the median value obtained from the counting of 100 random fields of view on three replicate slides,, and expressed as number of valves/phytoliths per gram of sediment. Due to the fact that diatoms have the hydrodynamic behavior of a silt particle, in cases where grain size is very variable, such as in this case, the final absolute abundances have to be corrected for the fine fraction w% content of each sample.

Geochemistry

For geochemistry analysis sediment samples were freeze-dried and grounded. Organic carbon (C_{org}), and calcium carbonate ($CaCO_3$) contents were measured on 2mg of sediment using a Leco CHNS 932. The C_{org} and N_{org} contents (wt.%) were determined by the difference between total and inorganic contents. Briefly, the combustion of organic carbon in the fraction < 2 mm for 3 hours at 400°C allows the subsequent measurement of inorganic carbon content. Both raw and combusted sample were analyzed two times. If the difference between 2 repeated sample measurements were lower than 0.10 wt.%, the average of both measurements is accepted as the correct value. Organic carbon content was obtained from the difference between total carbon and inorganic carbon contents. Calcium carbonate (wt.%) is equal to $8.33 \times C_{inorg}$.

Major (Al, Fe, Mg, Ca, Na, K, Ti and Mn) and trace (Ba, Cr, Cu, Pb, Sc and Zn) elements were determined by inductively coupled plasma optical emission spectrometry (ICP-OES) while Li, Rb and Sr were measured by inductively coupled plasma mass spectrometry (ICP-MS). All these determinations were obtained after total mineralization of 0.25 g of freeze-dried and ground sediment. The samples were mineralized by a combination of 3 mL HCl (36%), 9 mL nitric acid (HNO_3 ; 69%) and 5mL hydrofluoric (HF; 48%) in a CEM microwave oven Mars Xpress. After microwave digestion, remaining solutions were transferred to Teflon vessels and placed on the hotplate at 150°C until near dryness. Twenty mL of Milli-Q water and 2.5 mL HNO_3 were added to the residue to bring the solution to a final volume, the solution was heated at 80°C during 3 hours, and after cooling transferred to 50mL volumetric flask and finally poured in a labeled plastic bottle.

Quality assurance/quality control (QA/QC) concerns were addressed through the use of certified reference materials (CRM), blank reagents and duplicate samples. The accuracy of the analytical procedure was determined by measuring major and trace elements contents in three distinct CRMs (MAG-1 (USGS), PACS-2 and MESS-3 (NRCC); Table 2). Certified reference measured values are in general within the certified range of values, excepting Pb for MAG-1. The average recovery values for three replicate samples are listed in Table 2. The relative percent difference (RPD) was determined for duplicate samples of different studied samples to provide an indication of the analytical precision.

Values were generally precise within 10% (Figure 3). Duplicate samples with an RPD of greater than 20% were not considered in this work.

Table 2 - Average elemental recovery values in percentage for the 3 CRMs studied.

	PACS-2	MESS-3	MAG-1
Al	97	94	96
Fe	99	95	101
Mg	104	106	99
Ca	97	93	100
Na	103	102	107
K	110	99	101
Mn	101	95	97
Cr	99	97	102
Cu	106	95	90
Li	95	96	95
Ni	105	100	97
Pb	103	110	115
Sr	105	104	94
Zn	105	96	103
Ti	*	*	99
Ba	*	*	96
Rb	*	*	100
Sc	*	*	87

* certified reference values not available for these elements

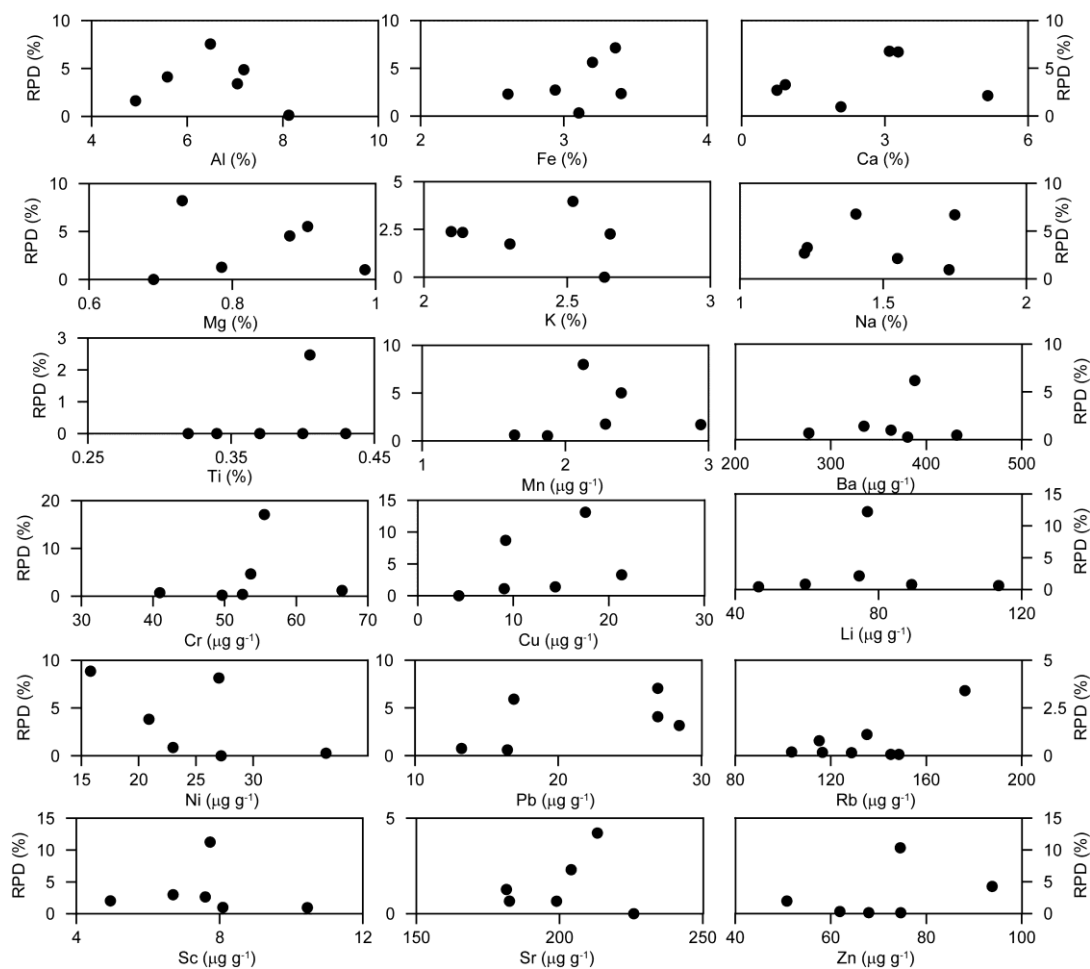


Figure 3 – Comparison of duplicate samples for studied elements.

Biomarkers

The analytical procedure started with sample preparation and lipids extraction. Sediment samples are freeze-dried and manually ground for homogeneity. From an aliquot of the dried material, the lipids are extracted by treating them three times with 8 mL of dichloromethane in an ultrasonic bath (15 min) after adding 10 µl of an internal standard containing *n*-nonadecan-1-ol, *n*-hexatriacontane and *n*-tetracontane. The extracts are combined and evaporated to dryness under a nitrogen flow. The evaporated extracts are hydrolyzed with 3 mL of 10% KOH in methanol and stored overnight for elimination of wax ester interferences. Non-acid compounds are recovered by extraction with *n*-hexane (3 x 3 mL). The resulting extracts are washed with extracted distilled water, evaporated under a nitrogen stream, and derivatized with 40-60 µl of N,O-Bis(trimethylsilyl)trifluoroacetamide (BSTFA) and diluted in toluene. Samples are stored in darkness at 4°C before gas chromatographic analyses (GC-FID, GC-MSD). An Varian gas chromatograph GC-8300 coupled with a flame ionization detector (GC-FID) using a capillary column (50 m length, 0.32 mm internal diameter) and hydrogen as carrier gas. Samples are injected on-column. After an initial period of 1 min at 90°C, the column is heated rapidly to 170°C at 20°C/min, then to 280°C at 6°C/min, followed by an isothermal period of 70 min, and a final temperature ramp of 10°C/min up to 310°C, and held for 5 min.

Quantification is performed by comparison of the peak areas with the area of the hexatriacontane peak. Sea Surface Temperatures (SST) determinations are based on the alkenone unsaturation index, U^{K}_{37} , which was calibrated to the temperature equation of (Muler et al., 1998). Replicate injections and sample dilution tests allowed assessing measurement errors below 0.5°C (Grimalt et al., 2001).

Pollens

Twenty seven (27) samples were analyzed from DIVA09. The treatment used for palynological analysis followed the procedure described by de Vernal et al. (1996), slightly modified at the UMR CNRS 5805 EPOC (Unité mixte de Recherche 5805, Centre National de la Recherche Scientifique/Environnement et Paléoenvironnements Océaniques) according to Desprat (2005).

Chemical digestion using cold HCl (at 10%, 25% and 50%) and cold HF (at 40% and 70%) were applied to eliminate carbonates and silicates. A *Lycopodium* spike of known concentration was added to each sample to calculate pollen concentration. The residue was sieved through 10µm nylon mesh screens (Heusser and Stock, 1984) and mounted in bidistillate glycerin. Pollen and cysts were identified and counted using a Nikon microscope with x550 and x1250 (oil immersion) magnifications. At least 100 pollen grains (excluding *Pinus*, aquatic plants and spores) and at least 20 pollen types were counted. *Pinus* pollen is usually over-represented in marine deposits and therefore is often

excluded from the main sum (Heusser and Balsam, 1977; Turon, 1984). However, it is known that the percentage of this *taxa* increase seaward in opposition to the decrease of total pollen contents (Muller, 1959; Bottema and Van Straaten, 1966; Groot and Groot, 1966; Koreneva, 1966; Van der Kaars and de Deckker, 2003). Because the site location is close to the present-day coast line, we assume that *Pinus* pollen percentages are not over-represented in this core and, therefore, *Pinus* pollen grains have not been excluded from the main pollen sum. Pollen percentages of each *taxa* were calculated based on the main pollen sum that excludes aquatic plants, pteridophyte spores and undetermined pollen.

Results

Chronostratigraphy

The age model for DIVA09 was defined based on 4 accelerator mass spectrometry (AMS) ¹⁴C measurements (Table 3), on ²¹⁰Pb analysis (Table 4; Figure 5a) and two historically dated botanical events in western Iberian Peninsula (Table 5; Figure 4).

The AMS ages were calibrated using CALIB Rev 6.0 program and the "global" marine calibration dataset (marine 09.14c) (Stuiver and Reimer, 1993; Hughen et al., 2004; Stuiver et al., 2005) (Table 4). The marine dataset (marine 049.14c) uses the global marine age reservoir correction (R) of 400 years for the Iberian margin as proposed by Bard et al. (2004) and a deltaR = -7 +/- -90 following (Reimer et al. 2004). We used 95.4% (2 sigma) confidence intervals and their relative areas under the probability curve, as well as the median probability of the probability distribution (Telford et al., 2004) as suggested by Stuiver et al. (2005). Two ¹⁴C dates from DIVA09 record exhibit age inversions, such as those obtained at 83 and 101cm core depth.

Table 4 - AMS radiocarbon measurements and calibration using CALIB Rev 6.0 program and the "global" marine calibration dataset (marine 09.14c) (Stuiver and Reimer, 1993; Hughen et al., 2004; Stuiver et al., 2005)

Lab code	Core depth (cm)	Material	Conv. AMS ¹⁴ C age BP	Conv. AMS ¹⁴ C age BP (-400 yr)	error	95.4 % (2σ) Cal AD age ranges	Cal AD age Median probability
KIA 42919	3	<i>snail</i>	465	65	25	cal AD 1689: cal AD 1949	1883
KIA 42920	57	<i>shell</i>	1730	1330	30	cal AD 466: cal AD 884	676
KIA 42920	83	<i>shell</i>	2380	1980	30	cal BC 329: cal AD 157	-55
KIA 42920	101	<i>shell</i>	2325	1925	30	cal BC 230: cal AD 258	11

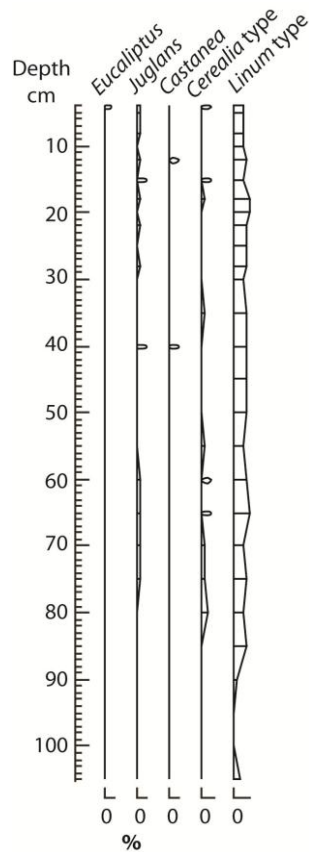


Figure 4 - Synthetic pollen diagram showing the introduced *taxa* in northwestern Iberian Peninsula.

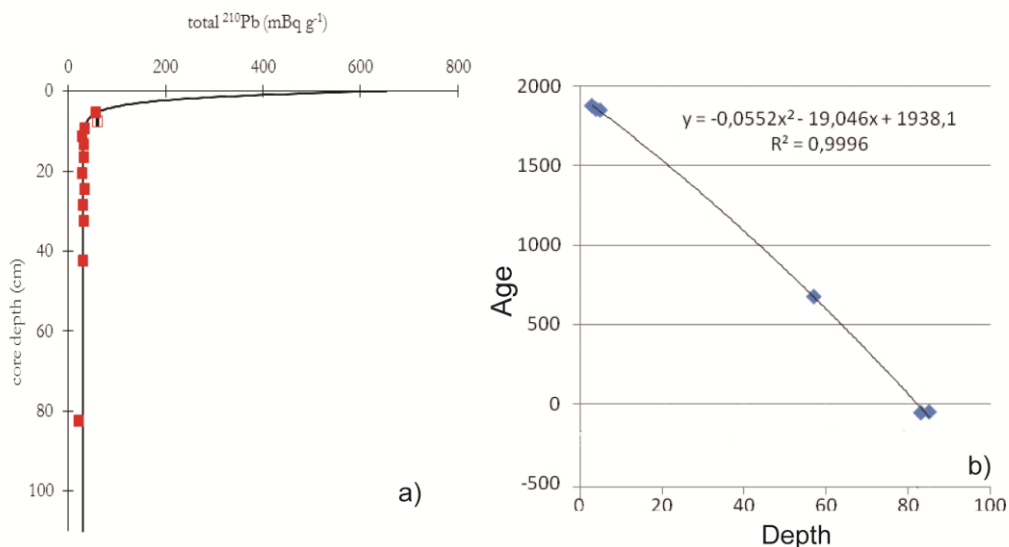


Figure 5 – Best-fit profile for ^{210}Pb results from DIVA09. The open square represent ^{210}Pb value not considered for determination of the sedimentation rate. Red filled squares represent background and unsupported ^{210}Pb activity. Horizontal errors bars are 1σ uncertainties propagated from counting statistics (a). Diamonds represent the accepted AMS radiocarbon ages. The independent second order polynomial adjustment is represented by the continuous dark line (b).

Two botanical events were detected in the synthetic pollen diagram (Table 5) and dated based on historical records. In particular, the appearance of *Juglans* occurred at ca. 50 yr BC (2000 yr BP) (85cm core depth) that was introduced by Romans (Carrion and Sanchez Gomes, 1992) during their settlement in the NW Iberian Peninsula (Desprat et al., 2003). The introduction of *Eucalyptus* in NW

Iberian Peninsula occurred at 1846 AD (CIDEU, Centro de Investigacion y Documentacion del Eucalypto; <http://www.uhu.es/cideu/caracteristicas.htm#Origen>). However, we added 10 years to this date because sexual maturity of Eucalyptus occurs around that age (Desprat et al. 2003). Therefore, the date 1856 AD was used for the level recording the first appearance of *Eucalyptus* in the pollen diagram (at 4cm). This hypothesis is in agreement with ^{210}Pb measurements.

Sedimentation rate (SR) was determined with the Constant Flux and Constant Sedimentation model (CF/CS model; Appleby and Oldfield, 1992 in Boer et al., 2006) using the solver function in Microsoft Excel ® on the basis of the least squares best-fit as described by Boer et al (2006). For analysis 12 samples were collected at different depths (Table 4). Due to ^{210}Pb half-life period, background levels of ^{210}Pb are known to occur at ~1850AD. In DIVA09 core, ^{210}Pb background values were found immediately below 10cm (values below 40 mBqg⁻¹ in the Portuguese Margin; according to de Stigter et al., 2007; Costa et al., 2011). Based on CF/CS, the estimated SR is about 0.05cm yr⁻¹ (Figure 5a). One value (7-8cm core depth, open symbol in Figure 5) was excluded when fitting the model curve, because it has a ^{210}Pb excess activity similar to the sample immediately above it, probably reflecting bioturbation or any other mixing process.

Table 4 – Samples used for ^{210}Pb measurements and quantity of ^{210}Pb and 1s error.

Sample depth	^{210}Pb (tot) (mBq g ⁻¹)	^{210}Pb 1s error (mBq g ⁻¹)	^{210}Pb 1s error (%)
5-6 cm	57.0	1.6	3
7-8 cm	57.9	1.6	3
9-10 cm	34.0	1.2	4
11-12 cm	28.9	1.0	4
13-14 cm	33.7	1.2	4
16-17 cm	32.6	1.1	3
20-21 cm	29.4	1.7	6
24-25 cm	34.6	1.7	5
28-29 cm	31.2	1.7	5
32-33 cm	32.8	1.7	5
42-43 cm	31.3	1.7	5
82-83 cm	22.6	1.3	6

Table 5 - Northwestern Iberia botanical events (according to Carrion and Sanchez Gomes, 1992, CIDEU, Centro de Investigacion y Documentacion del Eucalypto, Desprat et al., 2003).

Core depth (cm)	Age (yr AD)	northwestern Iberia botanical events
4	1856	<i>Eucalyptus</i> introduction
85	-50	<i>Juglans</i> development

For reconstructing our age model we have rejected the obtained AMS dated level at 101cm core depth since this date exhibit an age inversion being older than the overlying AMS date at 83cm core depth and the botanical event dated at 85cm core depth. After rejecting the outlying date, we considered the remaining 3 AMS ^{14}C dates, the two botanical dated events and ^{210}Pb results. A second order polynomial adjustment was applied to establish our age model (Figure 5b). The depth-age model

indicates that DIVA09 core covers the period from 670 cal BC to 1880 cal AD. During the 2500 yr record, the SR varies between 0.037 and 0.051cm yr⁻¹ (average: 0.042cm yr⁻¹). These SR allow high resolution analyses, and the sampling interval ranges from 19 and 140 yr (average 75 yr). Such a resolution is necessary to determine rapid climatic and environmental changes.

The age model determined based on ¹⁴C radioisotope measurements, pollen data and ²¹⁰Pb analysis provided a medium sedimentation rate of ca. 0.04 cm yr⁻¹ which is also in agreement with sedimentation rates known for the GMP (0.04 cm yr⁻¹ - Martins et al. (2006); between 0.05 and 0.4 cm yr⁻¹ - Lantsch et al.(2009b)).

Grain size

Grain-size analysis in DIVA09 showed a core-depth variation with finer sediments in top core levels and slightly coarser sediments at basal levels (Figure 6a). The coarsest samples, located below 100cm core depth, have more than 60% of sand. From 77cm to 100cm core depth, DIVA09 show sand percentages varying between 30% and 45%. Above that depth, sand contents were lower than 30%. Grain-size composition maintains approximately constant for the first 30cms (Figure 6a). Mud fraction is dominated by silt contents (Figure 6b). Despite the general increasing trend of clay contents towards the recent time, down-core variability is marked by periods of augments (e.g. ca. 800BC to 300BC; ca. 100BC to 600AD) followed by diminution (ca. 300BC to 100BC; 600AD to 800 AD). Table 6 summarizes the statistical parameters for grain-size classes in the DIVA09 core.

According to Shepard's classification (Shepard, 1954) and using the visual basic program developed by Poppe et al. (2008) to classify sediments, samples from DIVA09 are classified as clayey silt at the top to sandy silt at the bottom core varying progressively with core depth (Figure 7, Table 7). Two samples (DIVA09 70-71cm and DIVA09 92-93cm) are classified as sand-silt-clay.

Table 6 – Grain-size distribution statistical parameters (sand, silt and clay) in DIVA09. Sand (> 63 µm) results are based on all depth samples. Mud (< 63 µm, clay + silt) results were only analyzed on the 46 samples.

	% sand	% silt	% clay	% mud
minimum	3.4	23.3	6.5	29.8
average	22.2	56.0	24.4	80.7
maximum	70.3	67.7	37.0	96.1

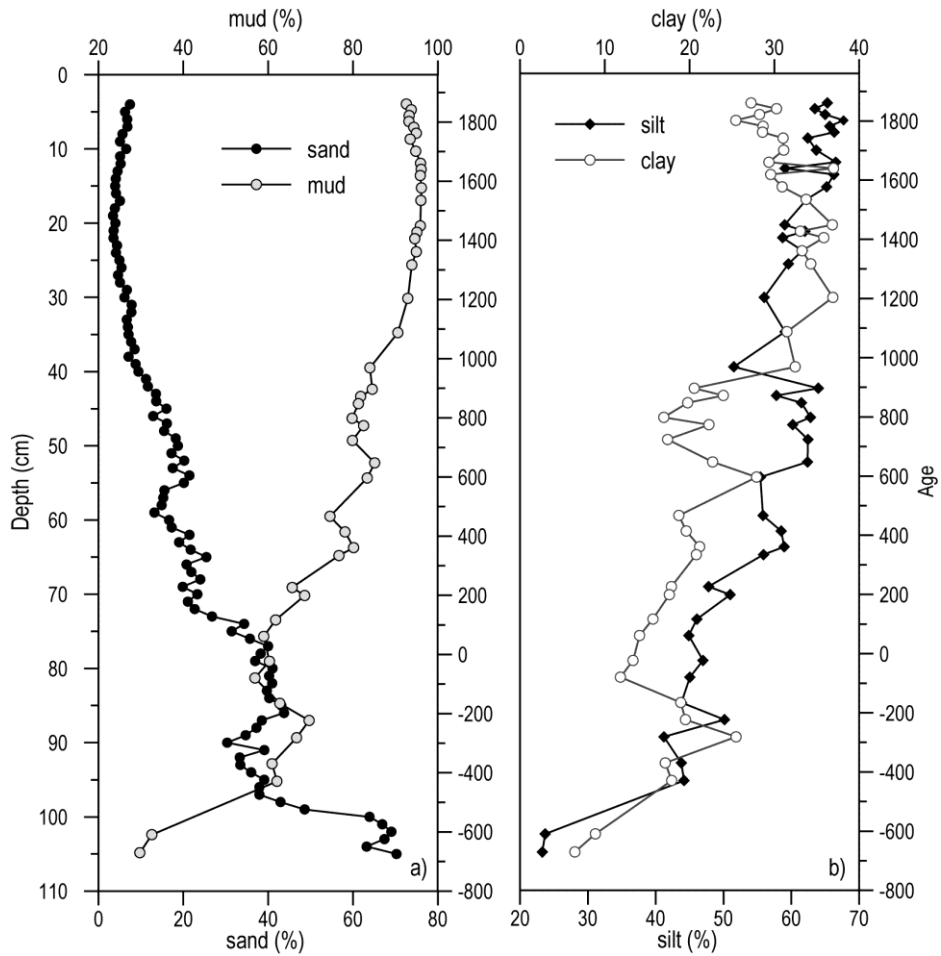


Figure 6 - Variation of grain-size with depth in DIVA09. a) Sand (> 63 μm) results are based in all depth samples. Mud (< 63 μm) results were only analyzed for the 46 samples where major and trace element analyses was also done. b) Clay and silt variability.

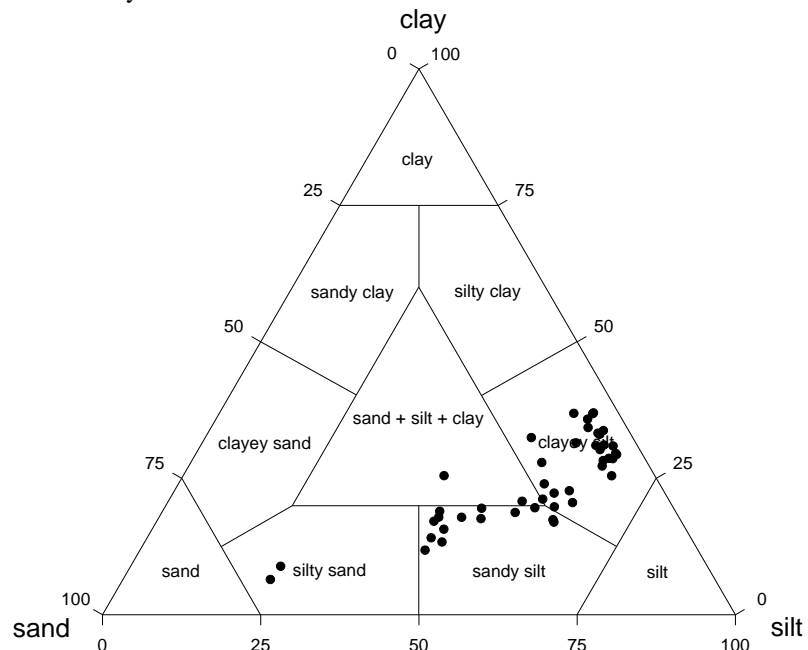


Figure 7 - Ternary plot of clay-silt-sand components from DIVA09. Field limits are from Shepard (1954). Only samples analyzed for geochemistry are presented in this plot.

Table 7 - Sediment classification from DIVA09. Classification defined by Shepard (1954) and visual basic program developed by Poppe et al. (2008).

Sample ID	% Sand	% Silt	% Clay	Shepard (1954) classification
DIVA09 4-5 cm	7.43	65.3	27.3	CLAYEY SILT
DIVA09 5-6 cm	6.26	63.5	30.3	CLAYEY SILT
DIVA09 6-7 cm	6.76	65.0	28.3	CLAYEY SILT
DIVA09 7-8 cm	6.83	67.7	25.5	CLAYEY SILT
DIVA09 8-9 cm	5.67	65.7	28.7	CLAYEY SILT
DIVA09 9-10 cm	5.08	66.3	28.6	CLAYEY SILT
DIVA09 10-11 cm	6.54	62.4	31.0	CLAYEY SILT
DIVA09 12-13 cm	5.22	63.7	31.1	CLAYEY SILT
DIVA09 14-15 cm	4.09	66.5	29.4	CLAYEY SILT
DIVA09 15-16 cm	3.94	59.1	37.0	CLAYEY SILT
DIVA09 16-17 cm	4.14	66.3	29.6	CLAYEY SILT
DIVA09 18-19 cm	3.87	65.2	30.9	CLAYEY SILT
DIVA09 20-21 cm	3.99	62.3	33.7	CLAYEY SILT
DIVA09 24-25 cm	4.13	59.0	36.8	CLAYEY SILT
DIVA09 25-26 cm	4.95	62.0	33.1	CLAYEY SILT
DIVA09 26-27 cm	5.44	58.7	35.8	CLAYEY SILT
DIVA09 28-29 cm	5.08	61.6	33.3	CLAYEY SILT
DIVA09 30-31 cm	6.13	59.6	34.3	CLAYEY SILT
DIVA09 35-36 cm	7.08	56.0	36.9	CLAYEY SILT
DIVA09 40-41 cm	9.43	59.1	31.5	CLAYEY SILT
DIVA09 45-46 cm	16.02	51.5	32.5	CLAYEY SILT
DIVA09 48-49 cm	15.46	64.0	20.5	CLAYEY SILT
DIVA09 49-50 cm	18.21	57.8	24.0	CLAYEY SILT
DIVA09 50-51 cm	18.73	61.5	19.8	CLAYEY SILT
DIVA09 52-53 cm	20.21	62.8	17.0	SANDY SILT
DIVA09 53-54 cm	17.50	60.2	22.3	CLAYEY SILT
DIVA09 55-56 cm	20.13	62.5	17.4	SANDY SILT
DIVA09 58-59 cm	14.89	62.4	22.7	CLAYEY SILT
DIVA09 60-61 cm	16.65	55.5	27.9	CLAYEY SILT
DIVA09 65-66 cm	25.43	55.8	18.7	SANDY SILT
DIVA09 67-68 cm	21.88	58.5	19.6	SANDY SILT
DIVA09 69-70 cm	19.86	59.0	21.2	CLAYEY SILT
DIVA09 70-71 cm	23.30	55.9	20.8	SAND SILT CLAY
DIVA09 74-75 cm	34.33	47.8	17.9	SANDY SILT
DIVA09 75-76 cm	31.40	51.0	17.6	SANDY SILT
DIVA09 78-79 cm	38.24	46.1	15.7	SANDY SILT
DIVA09 80-81 cm	41.03	44.9	14.1	SANDY SILT
DIVA09 83-84 cm	39.70	47.0	13.3	SANDY SILT
DIVA09 85-86 cm	43.12	45.0	11.8	SANDY SILT
DIVA09 88-89 cm	37.24	43.8	19.0	SANDY SILT
DIVA09 90-91 cm	30.34	50.1	19.5	SANDY SILT
DIVA09 92-93 cm	33.29	41.2	25.5	SAND SILT CLAY
DIVA09 95-96 cm	39.07	43.8	17.1	SANDY SILT
DIVA09 97-98 cm	37.93	44.2	17.9	SANDY SILT
DIVA09 103-104 cm	67.41	23.7	8.9	SILTY SAND
DIVA09 105-106 cm	70.25	23.3	6.5	SILTY SAND

Foraminifera

The planktonic $\delta^{18}\text{O}$ records indicate that hydrographic conditions at the DIVA09 site became more variable after 1300AD (Figure 8). The closeness between the $\delta^{18}\text{O}$ values of *G. bulloides* and *N. pachyderma* (r), both species related to upwelling along the northern Iberian margin (Salgueiro et al., 2008), indicates a well-mixed water column, most likely due to strong summer upwelling. Also between 300AD and 500AD, the water column was well-mixed during the summer months. On the other hand, between the core basement and 250 AD and between 600 AD and 950 AD the difference in the $\delta^{18}\text{O}$ data from both *G. bulloides* and *N. pachyderma* (r) reveal a more stratified water column. Conditions in the winter mixed layer as reflected by the species *G. inflata* were also more variable between 300AD and 500AD and after 1300AD with changes in the winter mixed layer often preceding

those changes in the surface layer. Salinity and temperature conditions in the bottom water, revealed by the $\delta^{18}\text{O}$ values of *Uvigerina* sp., were stable until ~1300 AD when two periods with colder bottom water occurred (1280-1350 AD and 1520AD – 1820AD).

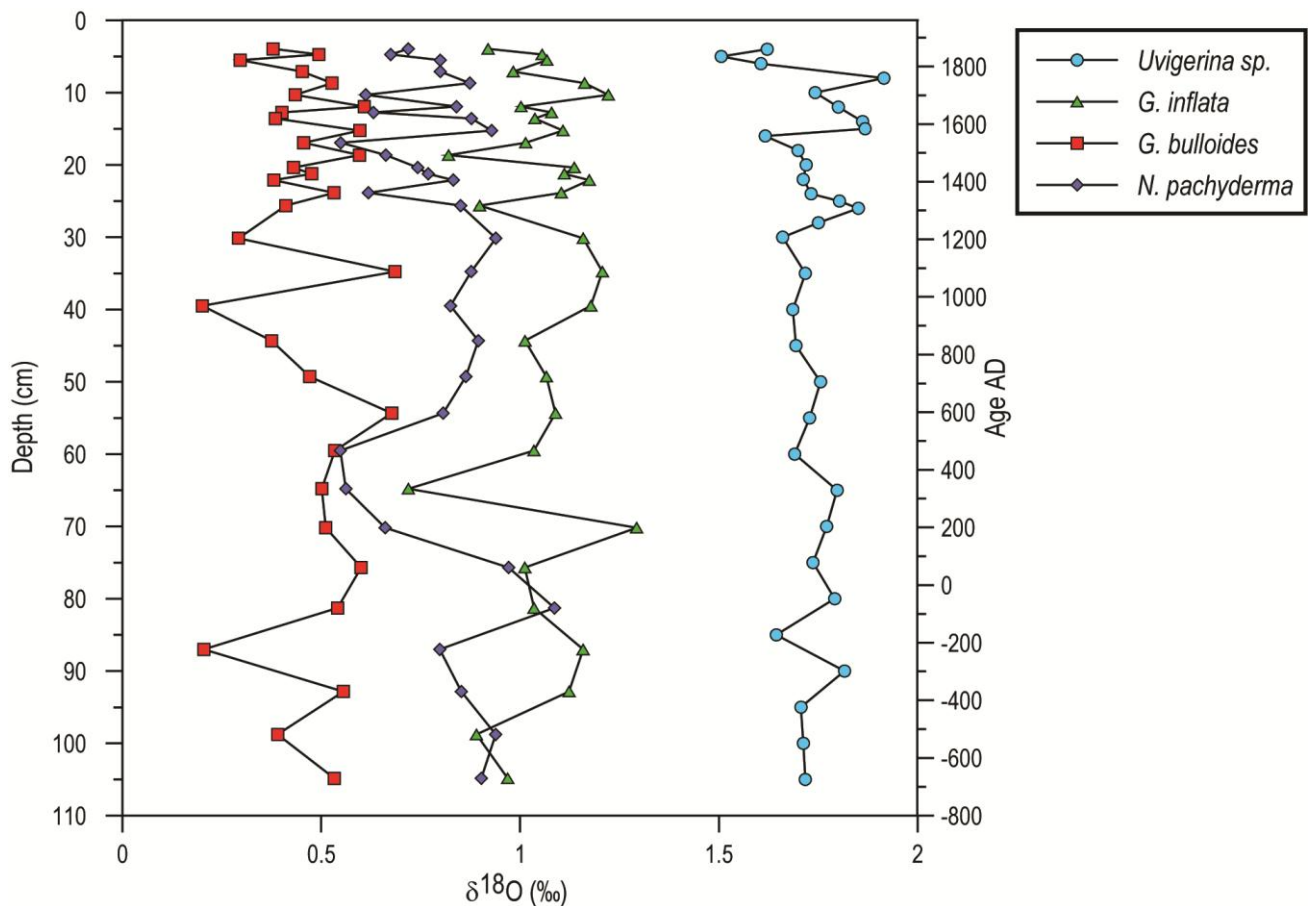


Figure 8 – Temporal variations of stable oxygen isotopes in 3 planktonic and one benthic foraminifera species.

Diatoms

The siliceous microfossils analysis reveals the presence of diatoms, phytoliths and sponge *spiculae*. Diatoms and phytoliths abundances through time are presented in Figure 9. Diatom preservation is generally poor, and only highly silicified taxa are present (*Paralia sulcata*, *Cocconeis* spp., *Diploneis* spp., *Chaetoceros* and *Leptocylinndrus* resting spores etc.). Diatom valves show signs of dissolution and only fragments were found at the following levels: 20-22cm (1535-1492AD), 32cm (1272AD) and 55cm (724AD). Levels barren of diatoms were found at 15cm (1649AD), 36cm (1181AD), 50cm (848AD) and 100-105cm (-519 to -670AD). Total diatom abundance is generally low ($< 5.04 \times 10^5$ valves g^{-1} , mean = 1.51×10^5 valves g^{-1} ; Figure 9a), which, suggests low productivity and/or bad preservation conditions. The predominant marine diatom taxa are (*Paralia sulcata*, *Cocconeis* spp., *Diploneis* spp., *Podosira* sp., *Thalassiosira* spp., *Chaetoceros* and *Leptocylinndrus* resting spores) in agreement with the coastal oceanic location of this site and possible cyclic influence of lower salinity waters. Centric diatom abundances show higher values than benthic diatoms (Figures

9b and c), tending to be predominant in the diatom assemblage record. *Chaetoceros spp.* resting spores (Figures 9d - red stars) are detected at sample depths 8cm (1782AD), 26-28cm (1406-1362AD), 60cm (597AD) and 75cm (199AD). *Leptocylindrus spp.* resting spores (Figure 9 - brown star) were only spotted at 4cm (1861AD).

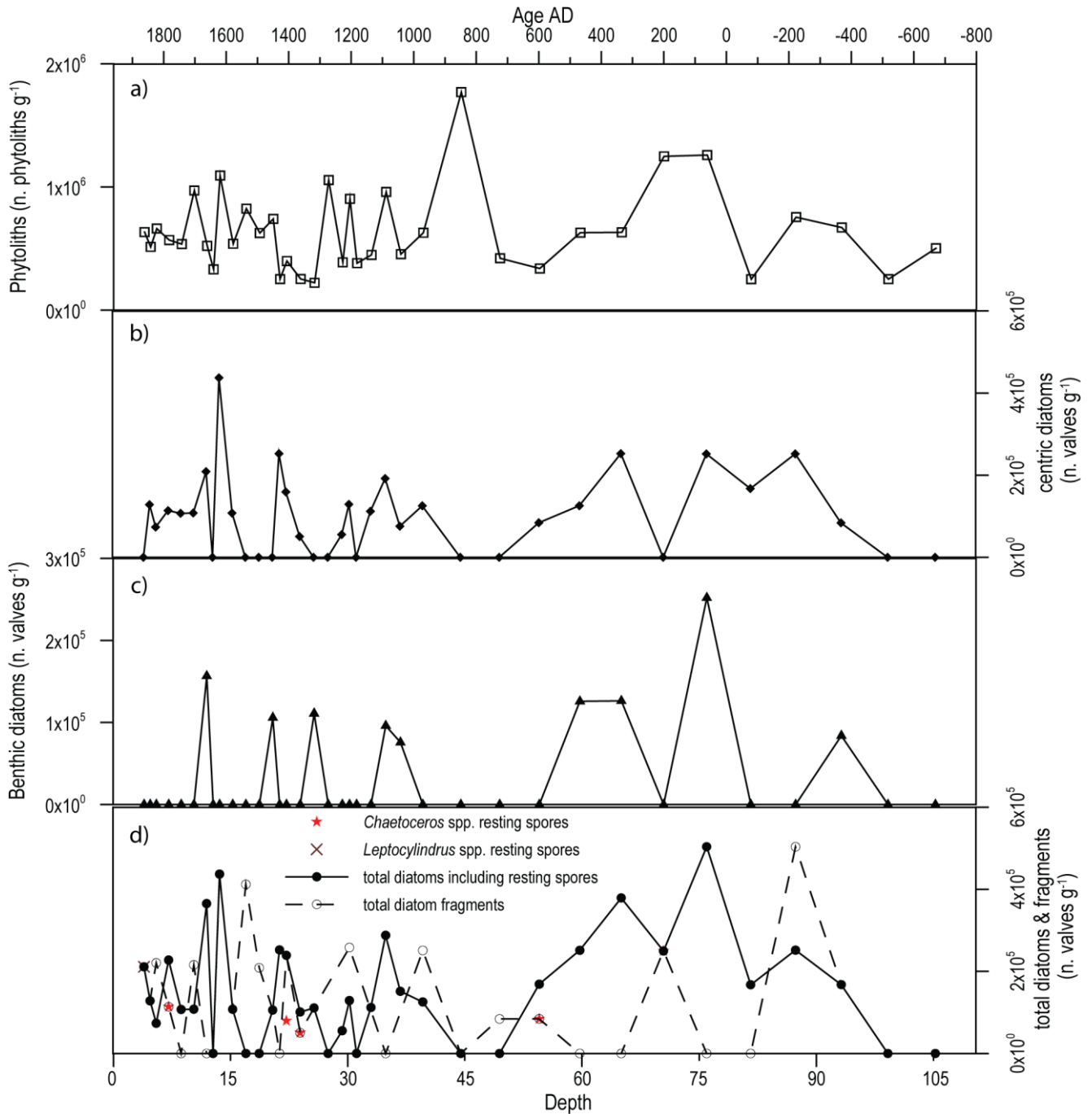


Figure 9 – DIVA09 siliceous microfossil abundance record vs. age. a) Total phytoliths abundance (n°. cells g⁻¹). b) centric diatoms abundance (n°. valves g⁻¹). c) benthic diatoms abundance (n°. valves g⁻¹). d) Total diatom abundance (including resting spores – solid line) and total diatom fragments (dashed line) expressed by number of valves or fragments g⁻¹ of sediment (n°. valves g⁻¹). Total resting spores abundance [*Leptocylindrus spp.* (brown star) + *Chaetoceros spp.* (red star) resting spores – n°. valves g⁻¹].

Phytoliths are observed all along this core, suggesting freshwater flux and transport of inland sediments derived from the northern Portuguese rivers (e.g. Douro, Minho) to this site, although freshwater diatoms were not detected. The total phytoliths abundance is generally higher than diatom abundance but within the same order of magnitude, and vary from 2.22 to 17.70×10^5 cells g^{-1} (mean = 6.39×10^5 cells g^{-1} ; Figure 9e). The high values of phytoliths may be related to a high resistance to dissolution of their silicate bodies.

Geochemistry

Organic carbon, total nitrogen and calcium carbonate

Organic carbon (C_{org}) and total nitrogen (N_{tot}) have similar down-core variability from the bottom to 300AD (Figure 10), where the highest C_{org} and N_{tot} values are found (Table 8). From this age until the top samples C_{org} decreases progressively, while N_{tot} contents decreases until 900AD. Above this age, N_{tot} values increases until 1000AD, and become approximately constant until top samples. Calcium carbonate ($CaCO_3$) varies from 1.3wt.% to a maximum of 13.4wt.%. It presents a slightly decreasing trend from the top until 1577AD. Below this, $CaCO_3$ values show a progressive increase with depth until 100BC, followed by another decrease until 400BC and a new increase below this age.

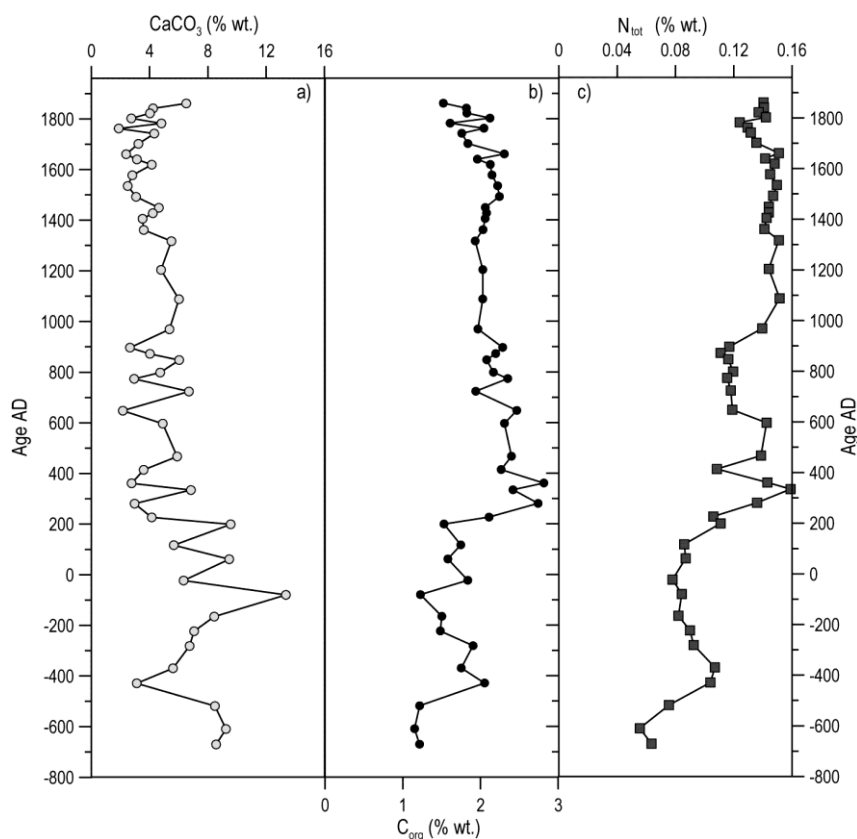


Figure 10 – Down-core variability of $CaCO_3$ a), C_{org} b) and N_{tot} contents c).

Table 8 – Organic carbon (C_{org}), total nitrogen (N_{tot}) and calcium carbonate ($CaCO_3$) distribution statistic parameters in samples from DIVA09.

	C_{org} (%wt.)	N_{tot} (%wt.)	$CaCO_3$ (%wt.)
minimum	1.2	0.056	1.9
average	2.0	0.122	5.1
maximum	2.8	0.159	13.4

Major and trace elements

Down-core variability of Al, Fe, Mg, K, Na, Ti and Mn concentrations are characterized by showing a similar trend marked by an increase between the core bottom (ca. 650BC) and 200BC followed by a short period where elemental contents slightly decrease until 100BC and a regular increase after this date (Figure 11). This similarity together with a strong linear relationship between all these elements ($0.73 < r^2 < 0.93$; Figure 12) suggests a common detrital origin; changes in the sediment supply; or, reflects the importance of mixing processes occurring during the transfer from riverine to the depositional areas at the shelf (e.g. currents, storms, waves).

Additionally, Li, Ba, Sc, Rb, Cu, Cr, Ni, Pb and Zn have down-core trends similar to the elements considered above as reflecting the fine-grained detrital sediment component (Figure 13). Increases in these elements clearly parallel the fine fraction, such as demonstrated by the strong relationships between Al, K and mud contents (Figure 12). Calcium and Sr present an inverse trend to all these elements being inversely correlated with Al (Figures 11, 12, 13, 14) indicating a distinct origin probably related to the sediment's biogenic component. The relatively low relationship between Ca and sand ($r^2=0.44$) suggests the occurrence of other minerals (e.g. quartz) at the sand fraction. Chromium, Cu, Ni and Zn are strongly correlated between each other (Figure 15) and with fine-grained proxies (Al and Li) (Figure 16) suggesting a common origin associated with fine-grained sediments. Lead is not so strongly associated with this set of elements (Cr, Cu, Ni, Zn, Al, Li; Figures 15, 16) suggesting other sources than that associated with fine-grained sediments.

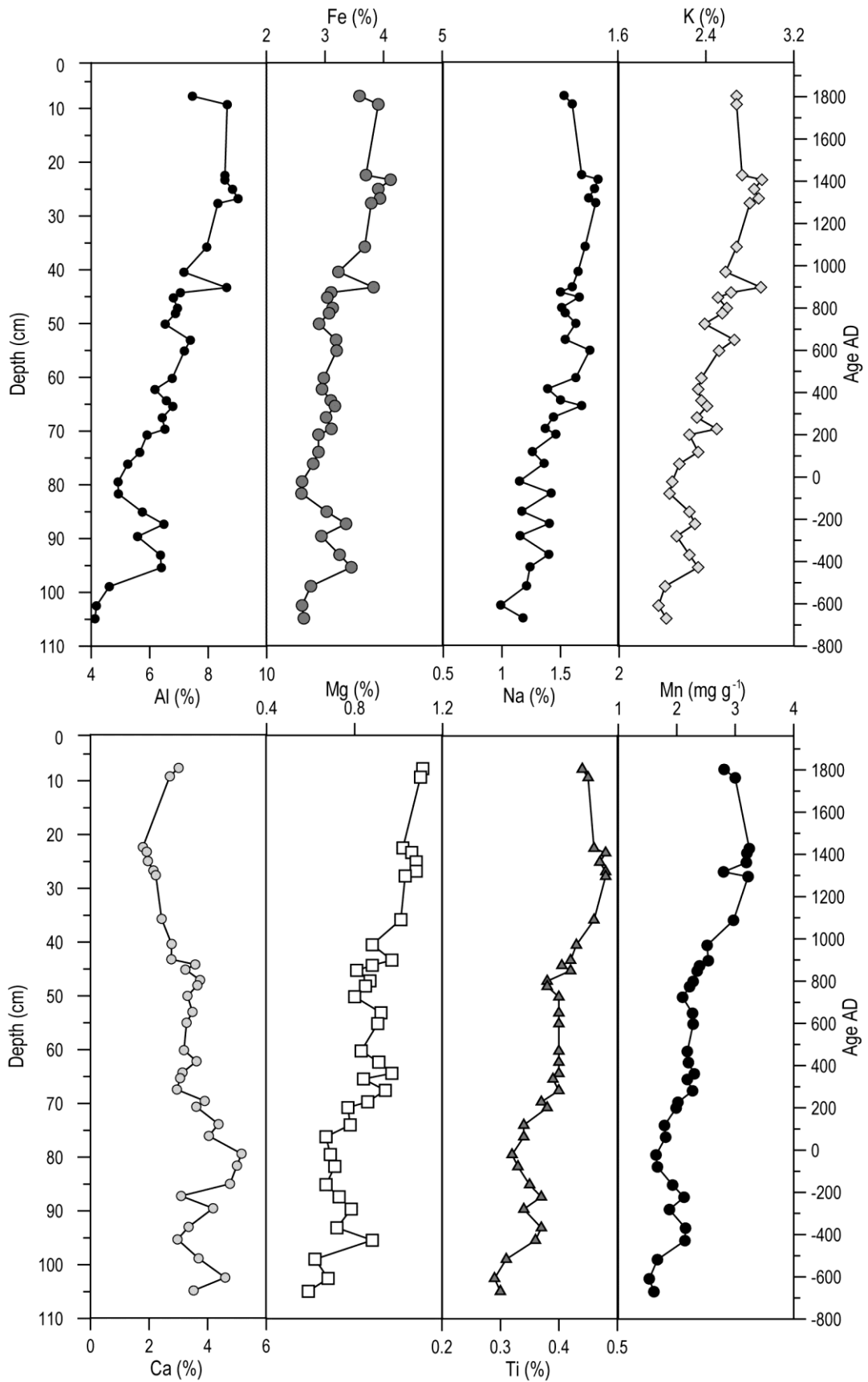


Figure 11 – Down-core variation of major elements concentrations.

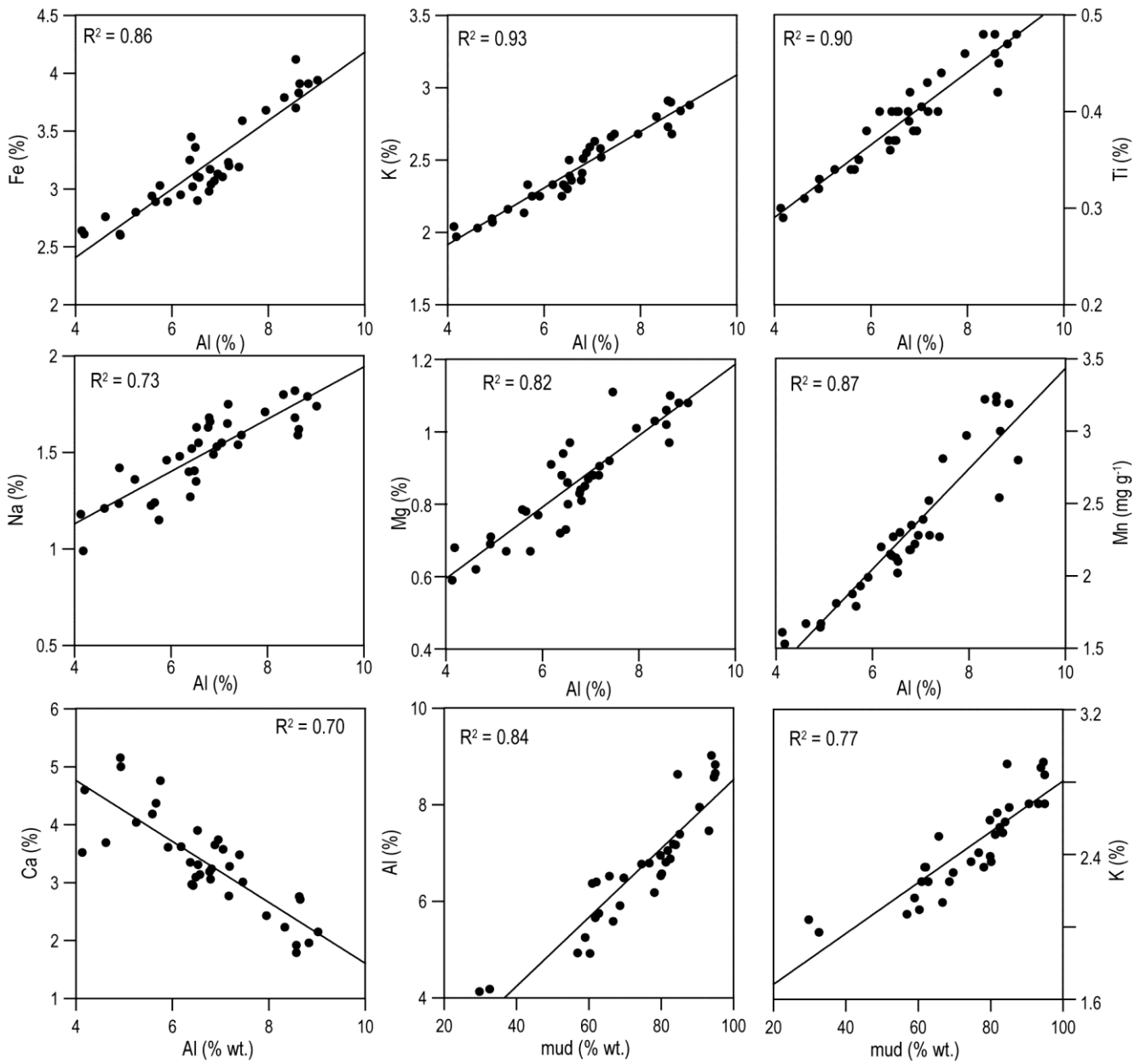


Figure 12 – Scatterplots showing the relationships between Al and the other major elements studied in DIVA09 core.

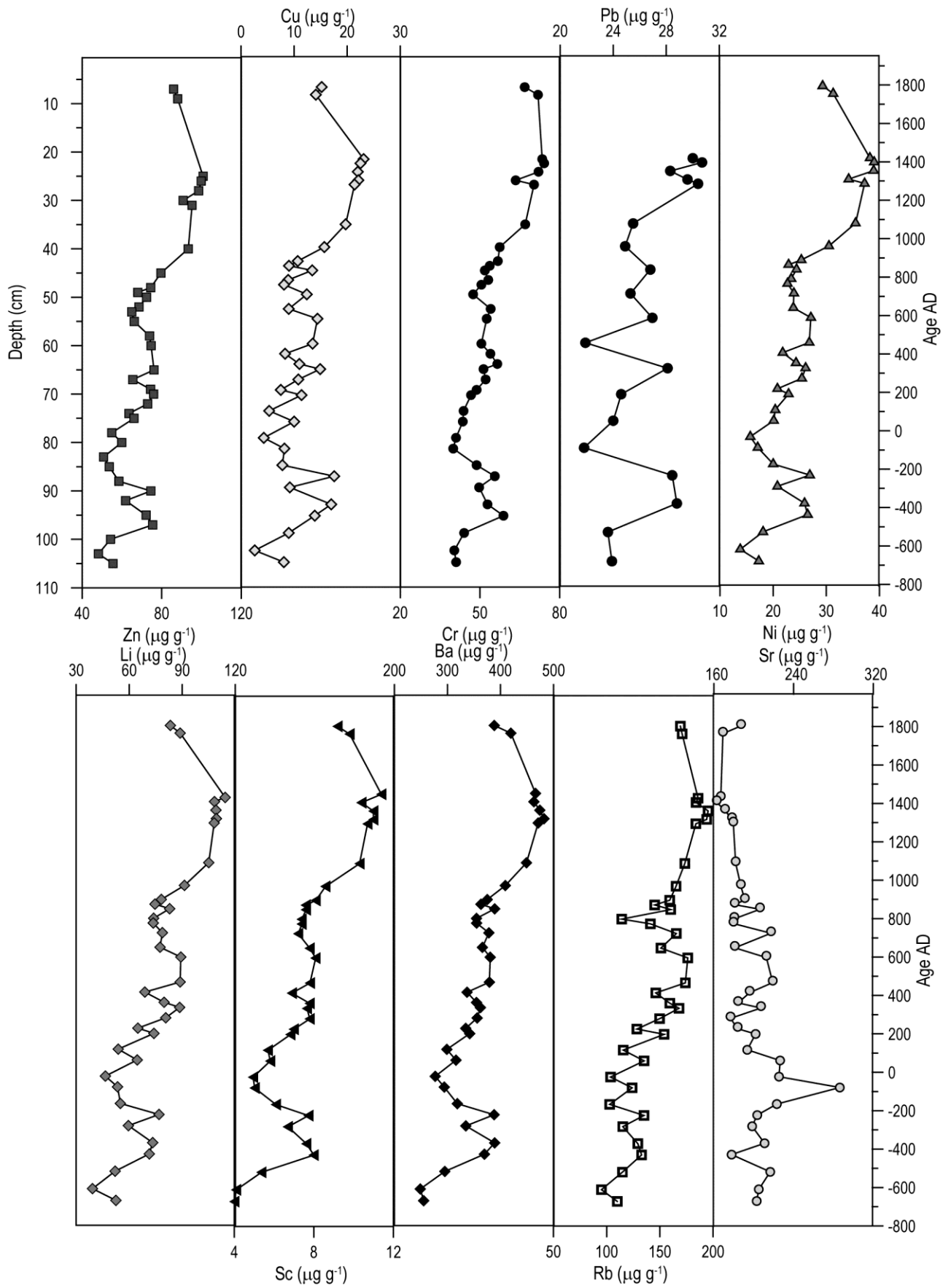


Figure 13 - Down-core variation of selected trace elements.

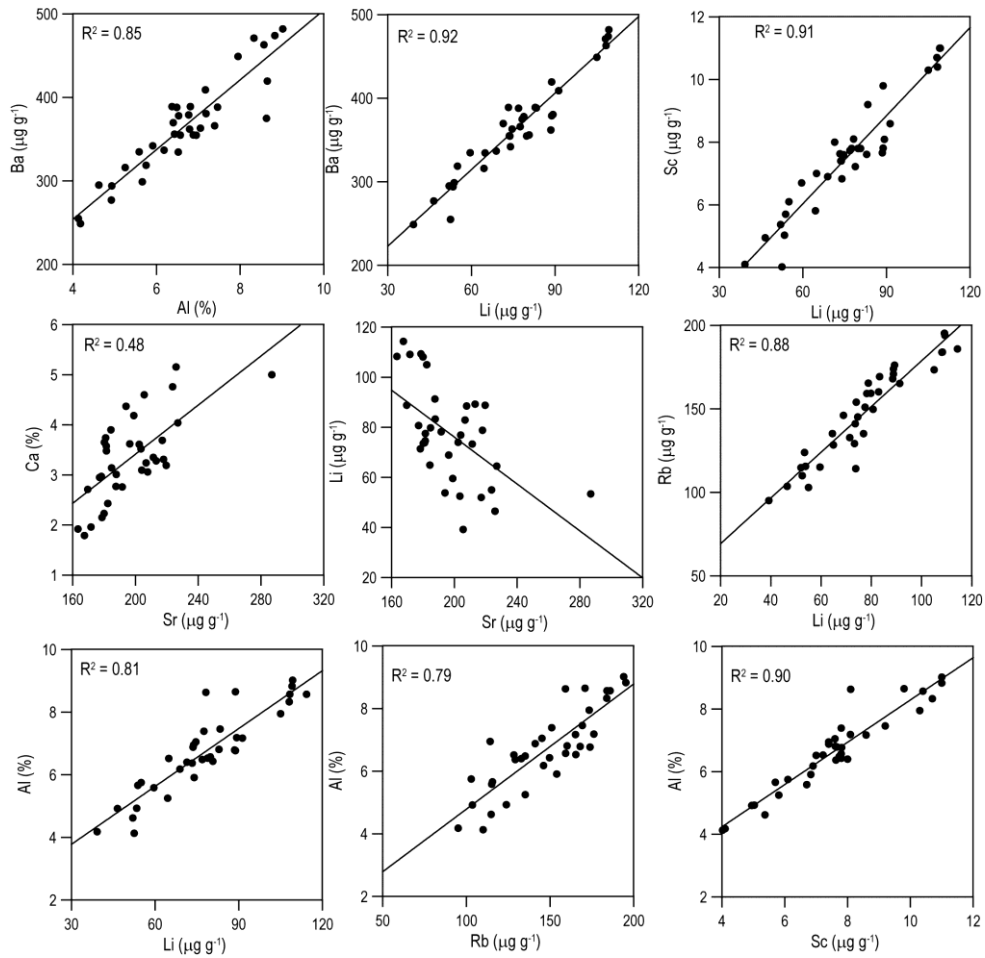


Figure 14 - Scatterplots showing the relationships between major elements (Al, Ca, K) and trace elements (Li, Sr, Rb, Ba, Sc).

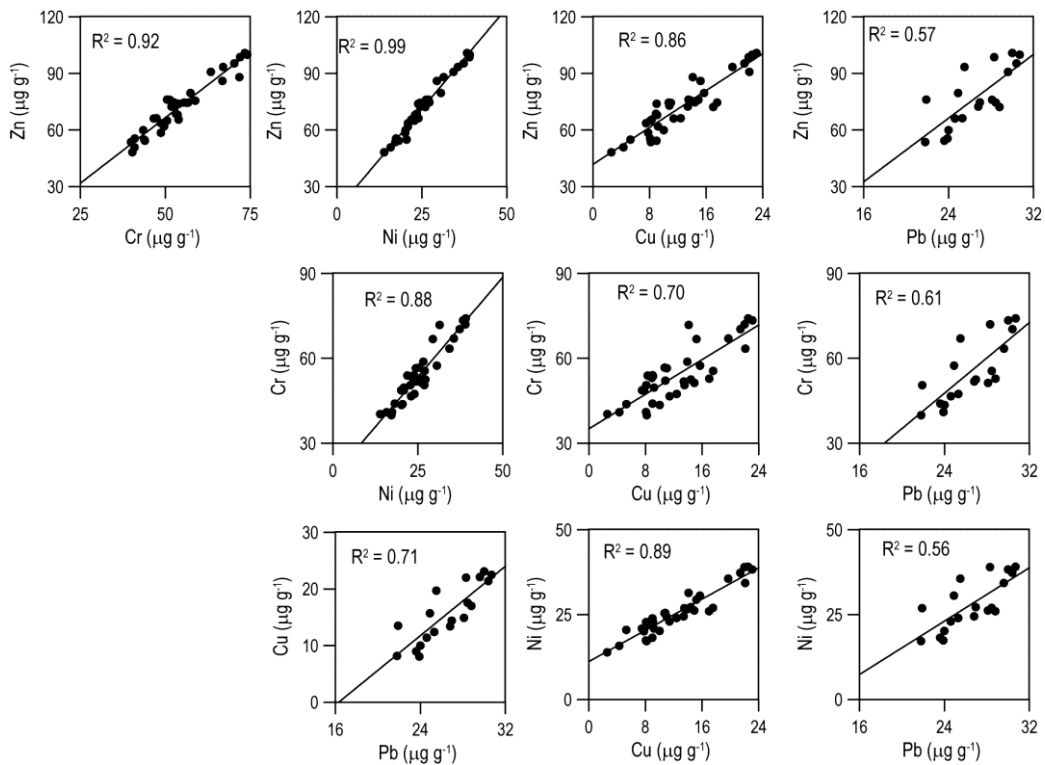


Figure 15 - Scatterplots showing the relationships between Cr, Cu, Ni, Pb and Zn.

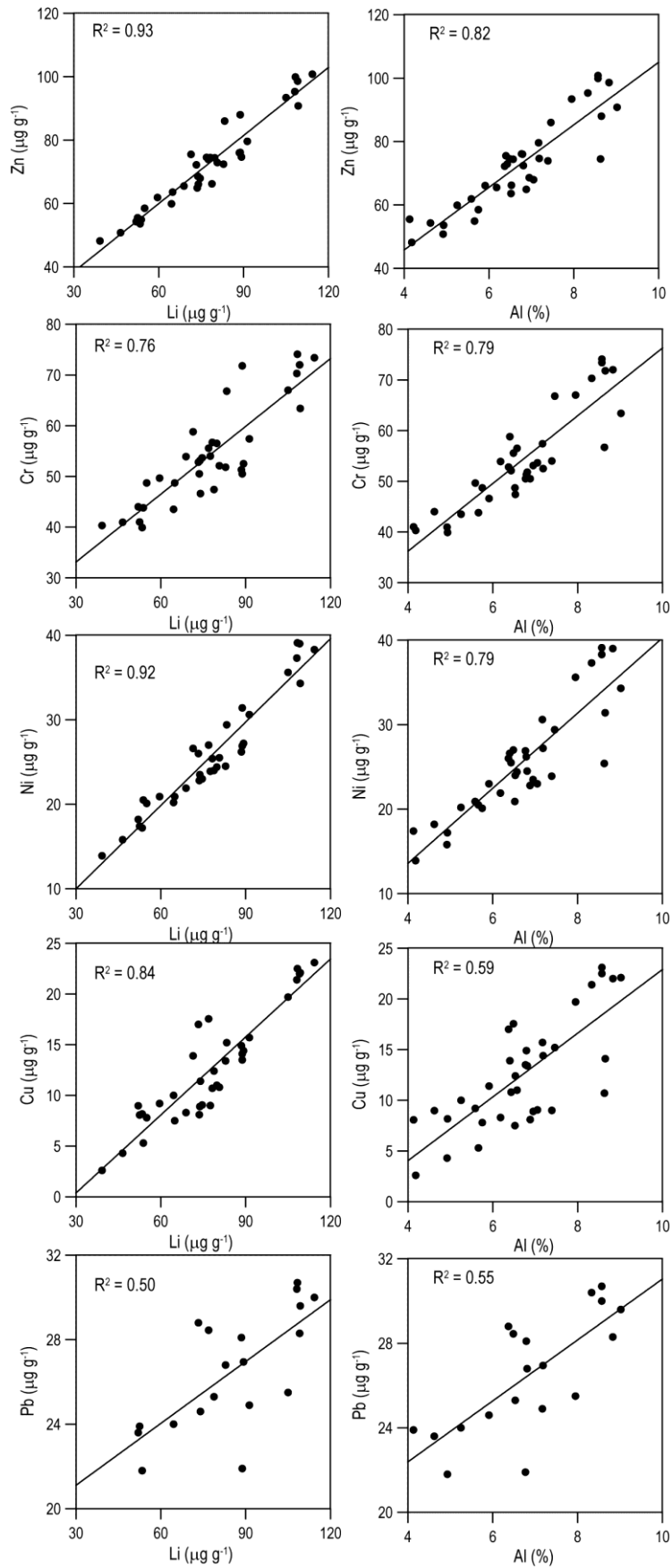


Figure 16 – Scatterplots showing the relationship between Cr, Cu, Ni, Pb and Zn with Li and Al.

Biomarkers

Sea Surface Temperature (SST)

Coccolithophores provide one of the geochemical tools most widely used to reconstruct past SST, based in the ketone unsaturated ratios. The ketone unsaturated ratios are believed to represent temperatures during production of long-chain alkenones by coccolithophores, and measurements from modern sediments indicate that the U_{37}^k index is a powerful tool for estimating past SST (Prah and Wakeham, 1987; Muler et al., 1998). The results of the SST based on alkenone analysis on DIVA09 core show maximum temperature values of about $\sim 17^\circ\text{C}$ in the bottom and temperatures close to 15°C in the top (Figure 17). The SST curve shows a gradual decreasing trend between 670BC and 1860AD, with the highest rapid variability over the last 700 years (i.e. from 1300AD to 1860AD).

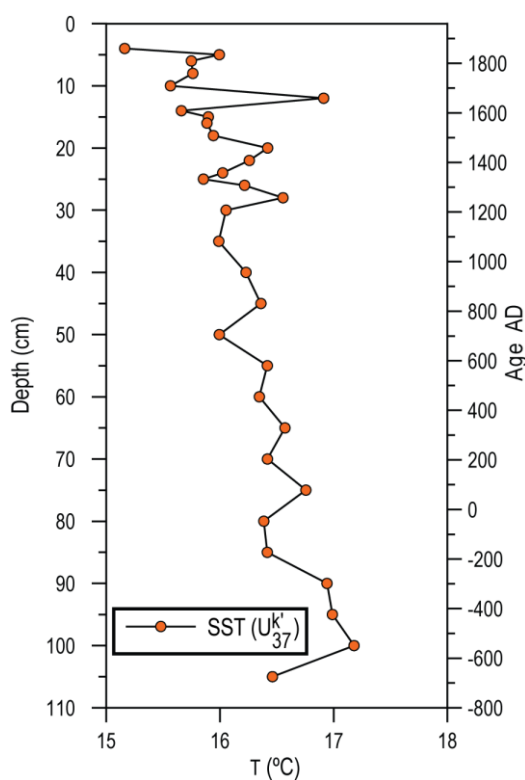


Figure 17 – Sea Surface Temperature (SST) results from the core DIVA09 vs. age.

Terrigenous biomarkers

Biomarkers are lipids of great utility in providing paleoclimatic informations. The *n*-alkanes and *n*-alkan-1-ols as allochthonous vascular plant debris (Eglinton and Hamilton, 1967) are indicative of terrestrial derived organic matter and show distributions dominated by even carbon number chain length. These plant waxes are easily removed from leaf surfaces by rain or wind, especially by sandblasting during dust storms. Molecular biomarkers are used to identify in sediment samples the occurrence of compounds with terrestrial origin (Figure 18). Thus the *n*-alkanes show maximum concentration of 3000 ngg^{-1} and the *n*-alcohols of 8000 ngg^{-1} , reflecting the maximum episodes of

terrestrial input. The results show in general an increase tendency until 1300AD and then a decrease to the top part. The concentration of *n*-alkanes and *n*-alkan-1-ols, clearly show an 200 yr length cyclicity.

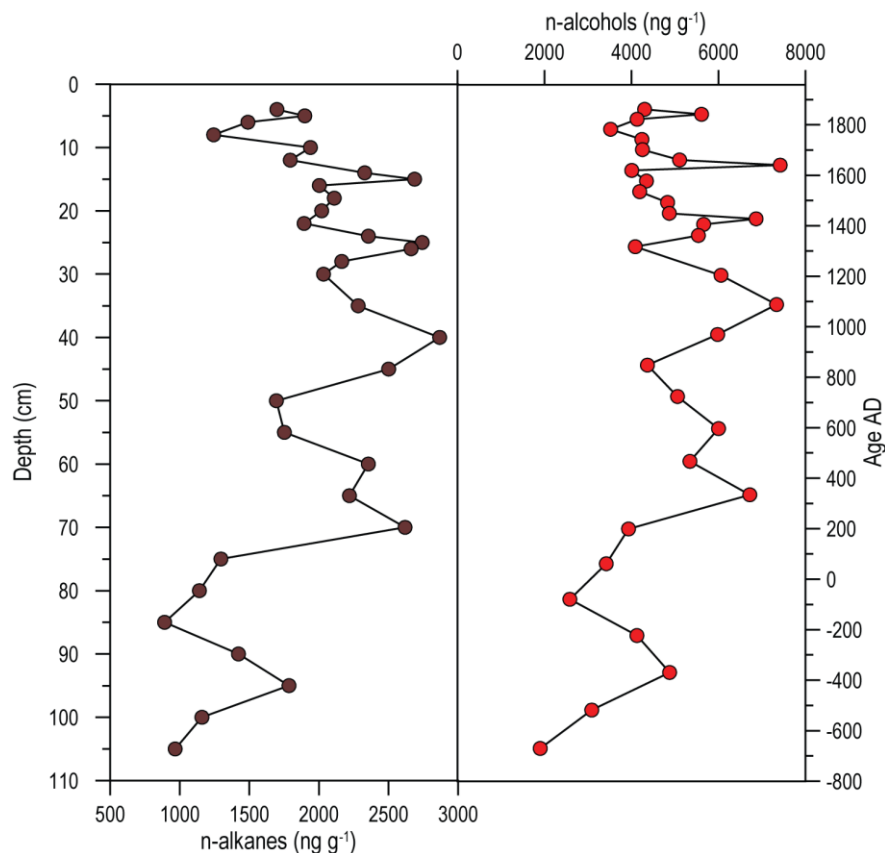


Figure 18 – Concentration of n-alkanes and n-alcohols along DIVA09.

Pollens

Pollen *taxa* were grouped into five ecological assemblages, each indicating different climatic conditions: temperate trees (including *Acer*, *Alnus*, *Betula*, *Corylus*, Cupressaceae, deciduous and evergreen *Quercus*, *Fraxinus excelsior*-type, *Pinus*, *Salix*, *Tilia* and *Ulmus*) recording a humid and temperate climate; the Mediterranean group (including *Cistus*, *Olea*, Evergreen *Quercus*, *Fraxinus ornus*, *Pistacia* and *Rhamnus*) recording warm and dry summers and cool and wet winters; the semi-desert plants (including Chenopodiaceae, *Artemisia* and *Ephedra*) recording dry conditions; the anthropogenic group (including *Juglans*, *Cerealia* type, *Olea*, *Castanea* and *Linum*) reflecting agriculture practices; and the ubiquist group (including all the pollen *taxa* excluding the temperate trees, Mediterranean, semi-desert and anthropogenic associations) which reflect relatively cool conditions or, alternatively, the development of pasture lands. Finally, the arboreal pollen (AP) group includes all the trees and shrubs and reflects temperature conditions. High AP increases reflect a climate warming while its decrease characterizes a decrease in annual temperature (Figure 19).

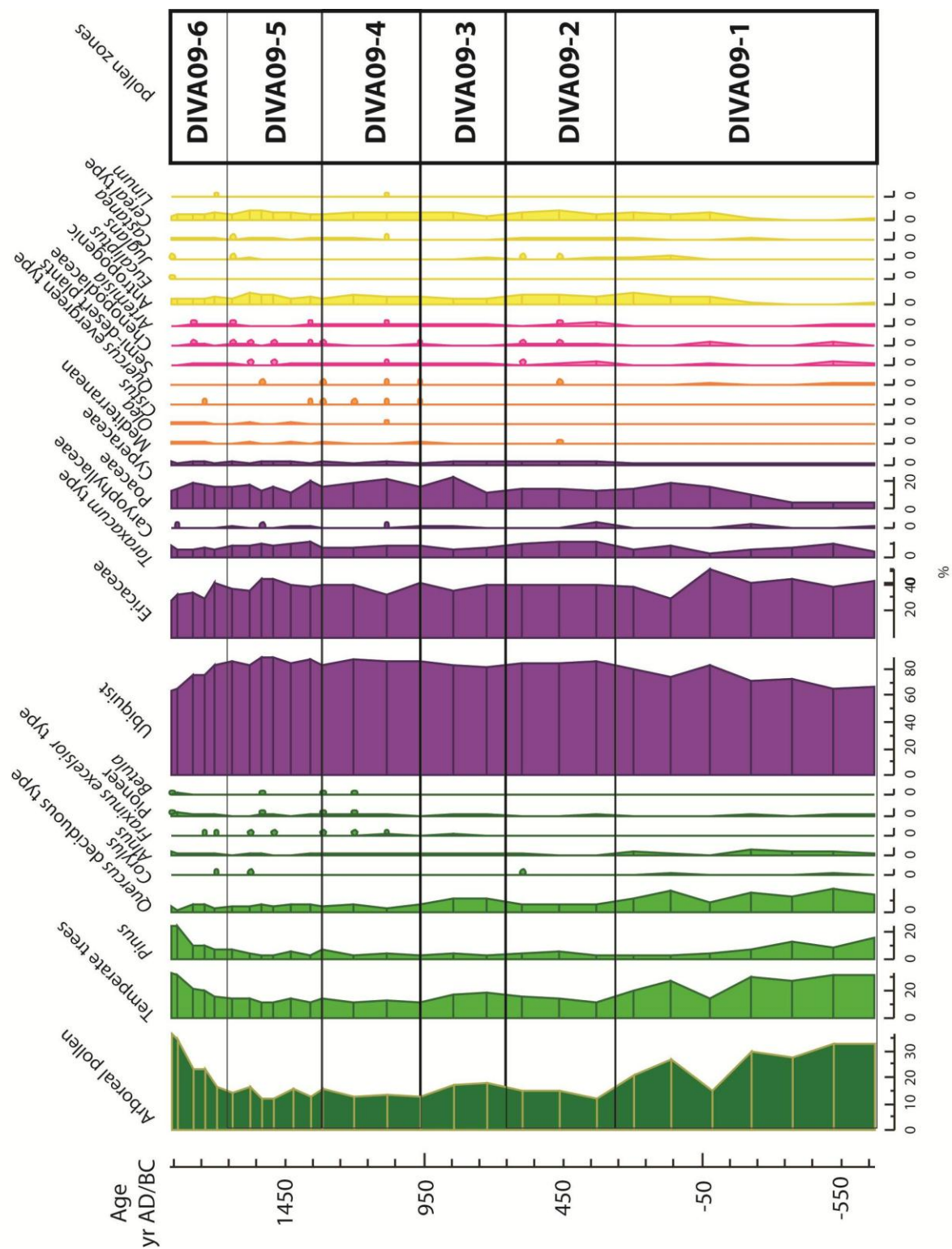


Figure 19 - Pollen diagram of core DIVA09.

The DIVA09 core records six main pollen zones numbered from the bottom to the top and prefixed by the abbreviated sequence name “DIVA09” (Figure 19). The establishment of these 6 pollen zones has been performed by using qualitative fluctuations of a minimum of 2 curves of ecologically important *taxa* or botanical groups (Pons and Reille, 1986).

The first pollen zone (DIVA09-1), 600BC-250AD, is marked by relative high percentages of temperate forest and in particular by deciduous *Quercus*, *Pinus* and *Alnus* forest and arboreal pollen which reflect warm and relatively wet conditions. The appearance of anthropogenic *taxa* is marked at 220BC reflecting the beginning of agriculture's practices in this region by romans. In particular, we note the beginning of the continuous presence of *Cerealia* since 220BC and also the appearance of *Juglans* at ca. 50BC. Both were also observed in the Ría de Vigo by Desprat et al. (2003).

The second pollen zone (DIVA09-2), 250AD-650AD, is marked by a decrease of AP and temperate trees and, in particular of deciduos *Quercus* and *Alnus*, and an increase of the ubiquitous group reflecting a relative climatic cooling. The slight increase in semi-desert plants suggest a relatively dryness of the continental conditions. However, this cooling and relatively dryness was not strong enough to perturb the agriculture practices that have started some centuries ago. This cooling has also been recorded in the Ría de Vigo identified by Desprat et al. (2003).

The third pollen zone (DIVA09-3), 650AD-950AD, is marked by a slight increase of temperate trees including deciduous *Quercus*, *Fraxinus excelsior* type and *Alnus* and a slight decrease of the semi-desert plants reflecting a relatively warming and slight increase of moist conditions. Although the climatic conditions were relatively better for agriculture practices there is a decrease in these *taxa*.

The fourth pollen zone (DIVA09-4), 950AD-1300AD, is marked by a slight decrease of temperate forest, the beginning of the continuous curve of Mediterranean *taxa* and increase of semi-desert plants. This suggests that there is a replacement of warm and wet conditions to a more Mediterranean climate which is characterized by warm and dry summers and cool and wet winters.

The fifth pollen zone (DIVA09-5), 1300AD-1700AD, is characterized by a similar pollen assemblage of the last pollen zone, but with relatively high percentages of ubiquitous and episodes of appearance and disappearance of semi-desert plants and of Mediterranean *taxa*. This suggests some instability of the NW Iberian Peninsula climate with extremely rapid or minor climate changes. In order to better understand what happened during this period we should study a higher resolution record should be studied. There are also two small episodes of increasing *Pinus* at around 1300 and 1450AD. The increase at 1300AD can be associated with two historical events, such as the plantation of a large area in Leiria region of pine trees by the Portuguese king D. Dinis (ca. 1310AD) and in other regions by the Cistercian monks for stabilizing sand dunes and soil protection, respectively (de Carvalho, 1960), and also for the use of pine wood for development of the naval industry (caravels and other types of seafaring vessels) during the era of Portuguese maritime expansion (around the 15 and 16th centuries).

Finally, the last pollen zone, (DIVA09-6), 1700AD-1880AD, is marked by an increase of *Pinus* percentages and therefore by an increase of temperate trees and AP associated with human activity. Indeed, it is known that the beginning of the continuous presence of *Pinus* forest has started 300 years ago (Queiroz and Mateus, 1994) and that they reach their maximum abundances in the last century as the result of successive deforestation policies (Valdès and Gil Sánchez, 2001).

Discussion

Temporal variability in organic matter composition

Organic matter constitutes (e.g. elemental C, N compositions, carbon and nitrogen stable isotope ratios, biomarker compounds) have been used to reconstruct marine and continental paleoenvironmental conditions (Meyers, 1997). The C_{org}/N_{tot} ratios have been used as a first approach to distinguish between marine (4-10) and continental (>20) origins of sedimentary organic matter (e.g. Meyers, 1994; Meyers, 1997). Intermediate values are usually found in marine systems close to land or in lakes, where mixing between terrestrial and aquatic organic matter occurs. Nevertheless, this elemental ratio can be affected by other sediment properties (e.g. grain size, proportion of inorganic nitrogen associated with clay minerals) and diagenetic processes. All these interactions may lead to a misunderstanding of organic matter sources (Cato, 1977). Also, in samples with low organic matter contents (< 0.3%) the C_{org}/N_{tot} ratios can sometimes be artificially depressed by a relatively large proportion of inorganic nitrogen (Meyers, 1997).

The regression between C_{org} and N_{tot} indicates that only 42% of N_{tot} is explained by C_{org} (Figure 20a), suggesting the presence of other nitrogen forms besides those associated with organic matter. This fact, together with the relatively high regression coefficient between N_{tot} and clays indicates a grain-size control of the nitrogen distribution (Figure 20b). The positive y-intercept in the N_{tot} and C_{org} relationship is interpreted indicating the presence of an inorganic nitrogen (N_{inorg}) component in the sediments (Schubert and Calvert, 2001). If the C_{org} and N_{org} linear regression is considered, the y-intercept is (0.005%), corresponding to a negligible fraction of inorganic N_{tot} (Figure 20c). As so, we used the total N_{org} fraction for the C_{org}/N_{tot} ratios calculations in order to avoid its overestimation (Schubert and Calvert, 2001). The N_{inorg} is probably bounded as ammonium ions to clay particles, especially illite (Stein and Rack, 1995) the dominant clay mineral in the northern shelf surface samples (Oliveira et al., 2002a). Organic carbon to N_{tot} ratios ranged between 11 and 24 with an average of 16, while C_{org}/N_{org} ratios lie between 16 and 29, with an average of 22 (Figure 21). The average ratios shift the interpretation of the organic matter from a mixed marine/terrestrial to a terrestrial source, with down-core trend revealing an increasing influence of terrestrial organic matter sources. Although this

interpretation is acceptable, it should be considered with some caution due to the influence of grain-size in C_{org}/N_{tot} ratios. According to Meyers (1997), high C_{org}/N_{tot} ratios were observed in coarser sediments. This grain-size effect seems well demonstrated if C_{org}/N_{tot} ratios are compared with sand contents (Figure 21). However, to corroborate this interpretation $\delta^{13}C$ should be measured in the future, because carbon isotopic ratios are not affected by grain-size variations and can be used to distinguish between marine and terrestrial (land plants, sewage) organic matter sources.

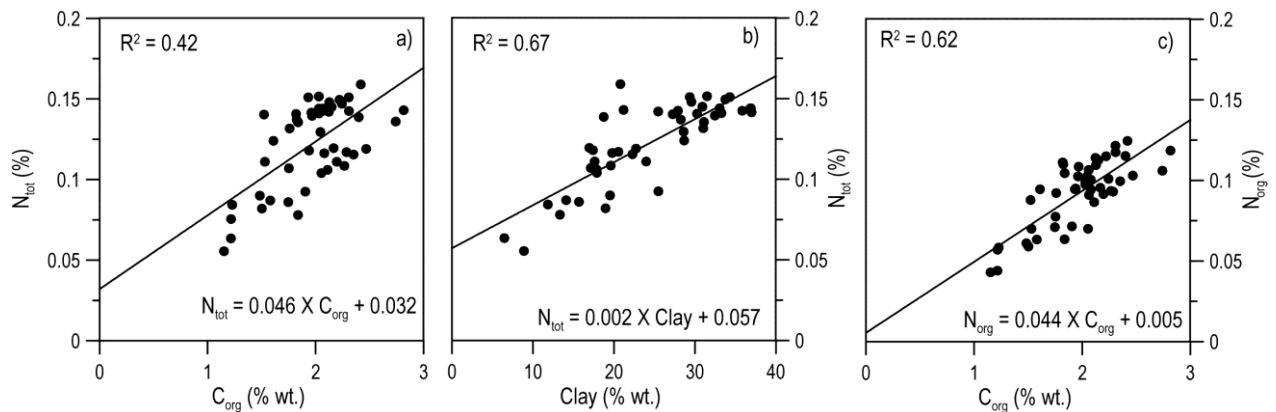


Figure 20- Relationships between total nitrogen (N_{tot}) and organic carbon (C_{org}) (a) and N_{tot} and clays (b) for the DIVA09 core samples. Data for C_{org} versus N_{tot} suggests the presence of inorganic nitrogen (N_{inorg}) bound in clay minerals. Correlation between organic nitrogen (N_{org}) and C_{org} (c).

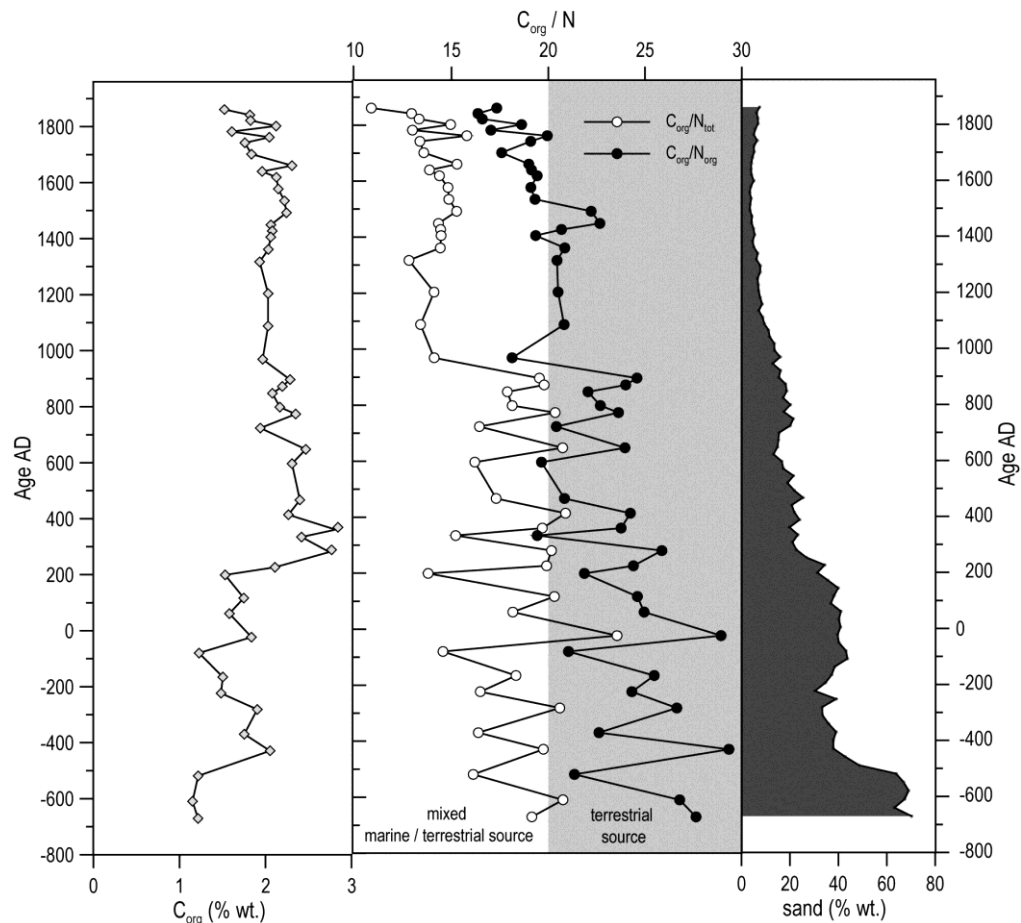


Figure 21- Down-core variability of organic carbon (C_{org}) compared with C_{org}/N_{tot} ratios determined from total nitrogen (N_{tot}) and organic nitrogen (N_{org}) and with sand contents.

Selection of the normalizer element

In order to compensate both grain-size and mineralogical variability affecting trace element distributions in sediments and also to identify anomalous contributions, geochemical normalization has been applied through the use of conservative elements strongly correlated with fine-grained sediments, such as Al (Windom et al., 1989), Fe (Schiff and Weisberg, 1999), Li (Loring, 1990) and Cs (Ackermann, 1980). Conservative elements are ideally derived from crustal rock sources, should have little or no effect from anthropogenic activities and be linearly correlated with other elements. Aluminum and Li are geochemically stable, not highly mobile, and also strongly correlated between them ($R^2=0.81$, Figure 14), and with both mud and clay contents (Figure 22). This suggests its coexistence in the lattice of fine-grained (clay, silt) particles. Furthermore, they are both correlated with most other studied major (Na, K, Ti, Fe, Mg, Mn; Figures 12 and 14) and trace elements (such as Ba, Cu, Cr, Ni, Rb and Zn; Figures 14 and 16). Despite Al and Li can be both used as normalizing elements, Al was chosen as a grain-size proxy because it has a relatively high value of R^2 with mud (Figure 22), which is interpreted as reflecting a major ability to normalize the other major and trace elements in relation also to different sediment grain size. Iron presents lower correlation coefficients than Al and Li with clay and mud contents ($R^2=0.66$ and $R^2=0.57$, respectively).

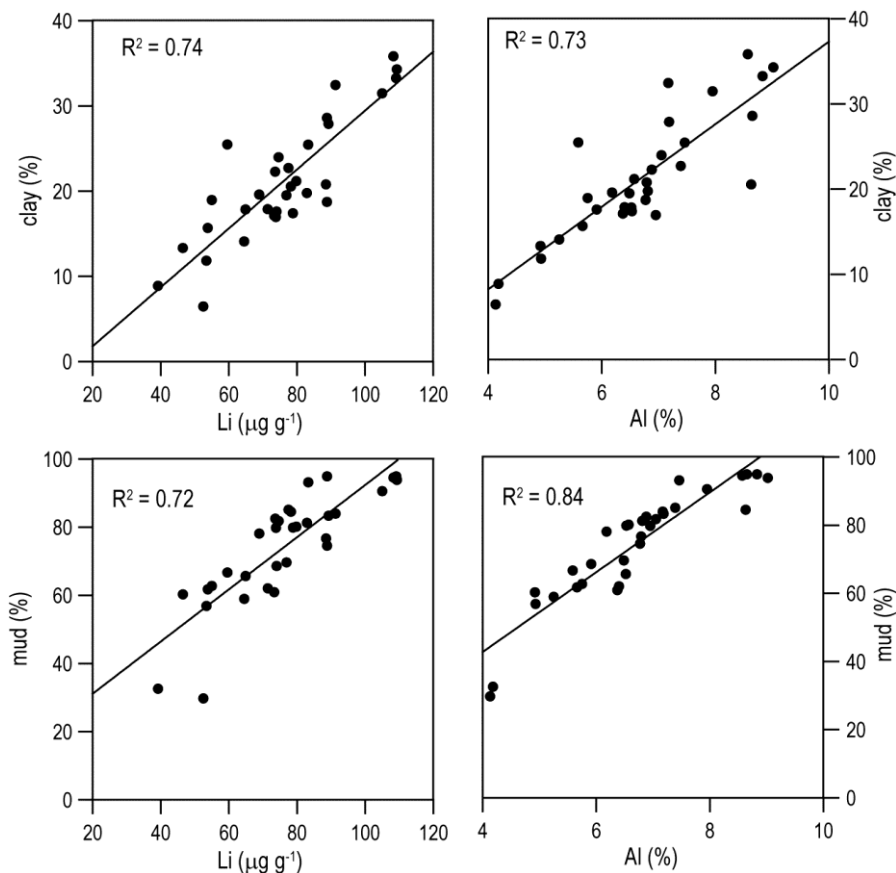


Figure 22 - Regression between Al and Li versus clay and mud in DIVA core sediments.

Temporal variability in supply of terrigenous materials

The variability of Fe/Al and Ti/Al ratios has been associated with changes in abundances of heavy minerals (e.g. amphibole, pyroxene, olivine, rutile, anatase). They can be interpreted as reflecting the strength of the sediment transport process (Zabel et al., 1999; 2001) and/or the energy of river discharges. Potassium is mostly associated with potassium feldspar, illite (Yarincik et al., 2000) and micas. K/Al ratios have been used as a proxy for intensity of chemical weathering (strongly affected by climatic parameters, principally rainfall and temperature), with high ratios indicating the dominance of physical weathering (Schneider et al., 1997).

Temporal variability of K/Al, Fe/Al and Ti/Al ratios presents the same increasing trends with depth characterized by high ratios on bottom levels (Figure 23), suggesting major abundance of heavy minerals and potassium feldspar. This mineralogical association can result from high energetic environmental shelf conditions (which should not allow the deposition of fine particles), and/ or associated with an increased level of precipitation that may be responsible by high river discharges and consequently a major efficiency on the transfer of large grain size terrigenous materials to the shelf, or both hypothesis. The high abundances of pollens derived from temperate forest (Figure 19) and major terrestrial source contributions derived from C_{org}/N_{tot} ratios (Figure 21) on these same levels seem to imply the occurrence of precipitation. Nevertheless, it is important to emphasize that temperate conditions evidenced by pollen data are not warm and wet enough to shift the prevailing physical weathering conditions to chemical weathering conditions, such as found in tropical and humid areas, as also indicated by the dominance of illite in surface sediments of the northern shelf area (Oliveira et al., 2002a).

Other trace elements (e.g. Cr, Cu, Ni, Pb and Zn) are released to the environment by natural processes and anthropogenic activities. These elements have been used by Man in their activities for thousands of years in distinct applications (e.g. manufacturing of materials, health applications, fossil fuel burning and mining) (Patterson, 1972; Nriagu, 1996). The anthropogenic impact started during the Greek and Roman times, but is the Industrial Revolution that corresponds to the historical period where considerable increments in the use of these elements resulted in a significant release into the environment (Nriagu, 1996). The depth profiles for elemental normalized ratios to Al (open circles, Figure 24) do not show any increasing trend towards the top sediments (normally interpreted as reflecting anthropogenic contributions) suggesting that increasing trends on total elemental variations (filled circles, Figure 24) are predominantly reflecting grain-size variations.

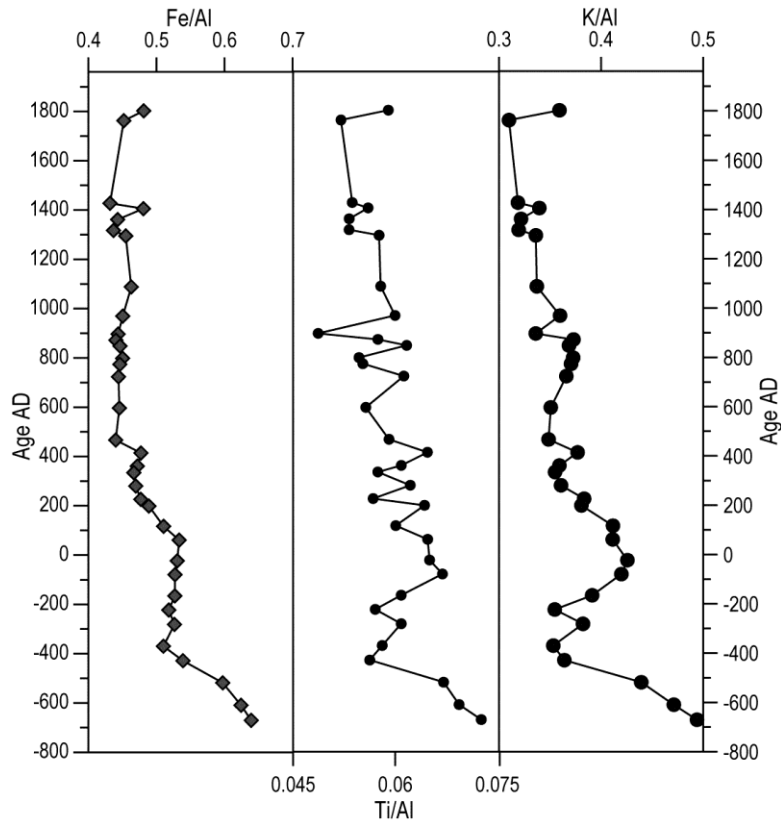


Figure 23 – Temporal variability of elemental indices of chemical weathering.

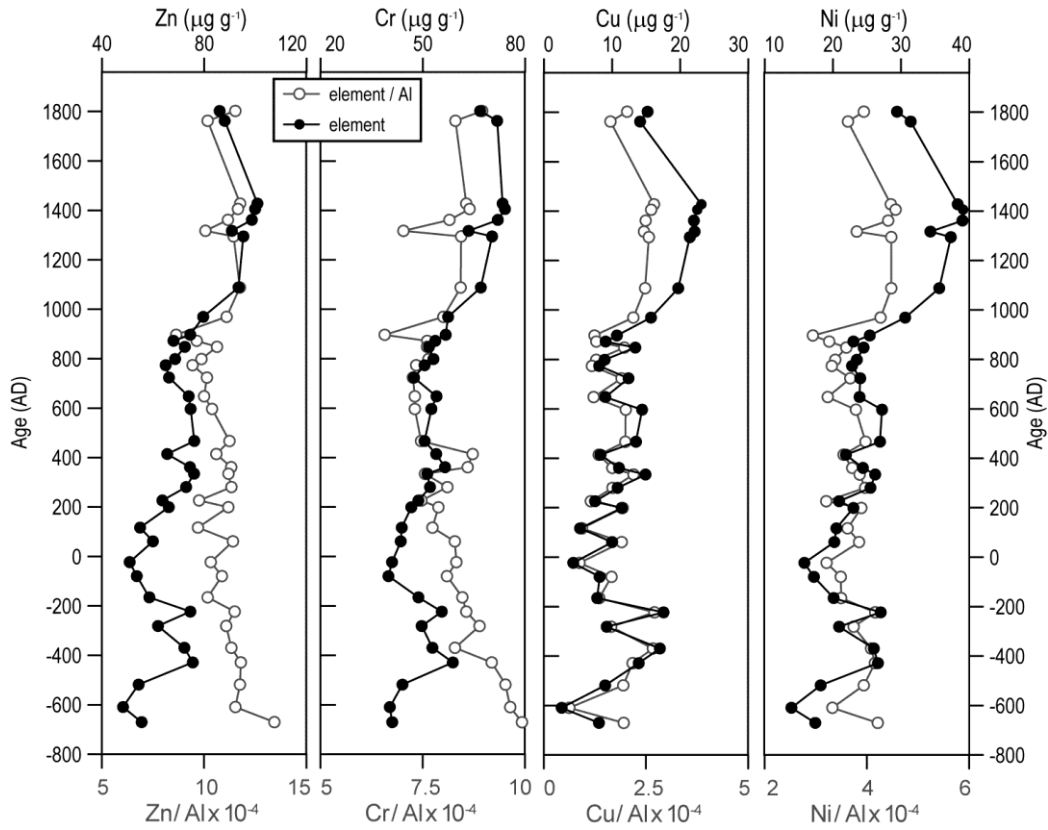


Figure 24 - Vertical profiles of total element (Zn, Cr, Cu and Ni) concentrations and element ratios to Al in the DIVA09 core.

Climatic changes in the NW Portuguese Margin and the influence of human activities since the last 2500 years

$\delta^{18}\text{O}$ -isotope composition of the NorthGRIP ice-core (Johnsen et al., 2001) and the decrease of mid-latitude summer insolation (after Berger, 1978) during the late Holocene (Figure 25) are in agreement with the previous suggestion that forest recession through the Holocene might be mainly the result of natural processes (Magri, 1995).

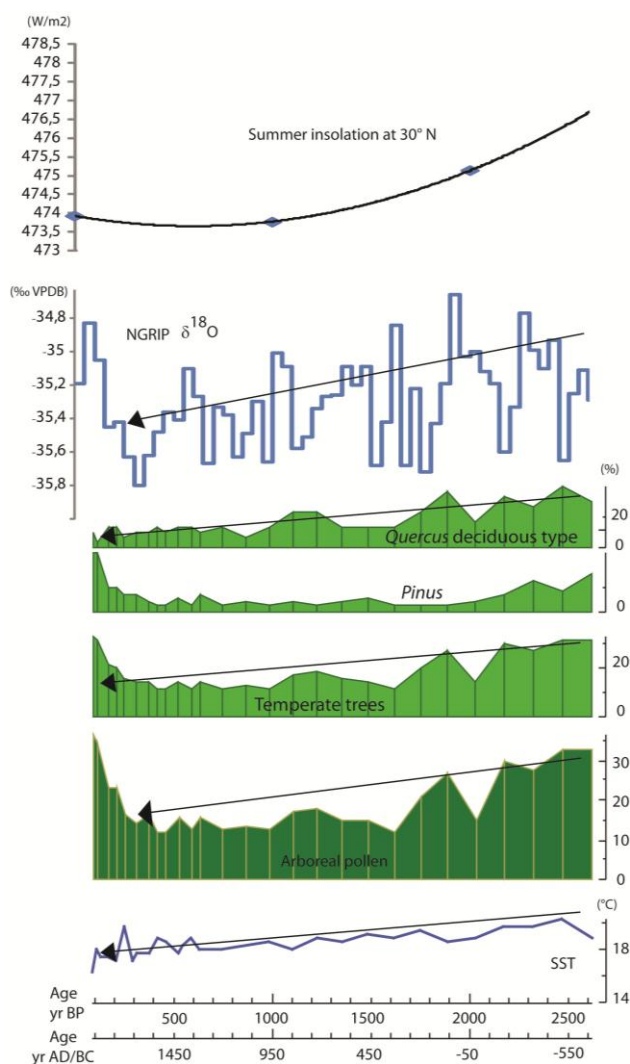


Figure 25 - Vegetation changes and quantitative Sea Surface Temperature (SST) variability in northwestern Iberian Peninsula and margin correlated with summer insolation at 30° N (after Berger, 1978) and $\delta^{18}\text{O}$ -isotope composition of the NorthGRIP ice-core (Johnsen et al., 2001) during the late Holocene.

Previous studies of sea-surface conditions of the North Atlantic and Mediterranean regions have shown an apparent long-term cooling trend driven by northern high latitudes summer insolation decreased during the Holocene (Marchal et al., 2002; Andersen et al., 2004; Moros et al., 2004, Rodrigues et al 2009). Several climate models also suggested an orbitally-induced mechanism as the main forcing factor for the long-term climatic trend over the Holocene (Kutzbach and Gallimore, 1988; Crucifix et al., 2002; Weber and Oerlemans, 2003; Renssen et al., 2005). Other authors (e.g.

Lorenz et al., 2006), have compared global alkenone-derived SST data with transient climate simulations using a coupled atmosphere-ocean general circulation model (AOGCM) for the last 7000 yr cal BP (less instable climate period) suggesting that mid- to late Holocene long-term SST trends were driven by insolation changes. Although SST gradually decreases up to nowadays, there is an increase in arboreal pollen and temperate trees percentage resulting from the increase of *Pinus* induced by successive reforestation policies (Valdès and Gil Sánchez, 2001).

Sub-orbital climate variability during the late Holocene

Superimposed onto the orbitally induced long-term cooling pattern, all the different proxies analysed from the DIVA09 shelf core including pollen, SST and planktonic $\delta^{18}\text{O}$, allow identifying sub-orbital climatic variability during the last 2500 years (Figure 26).

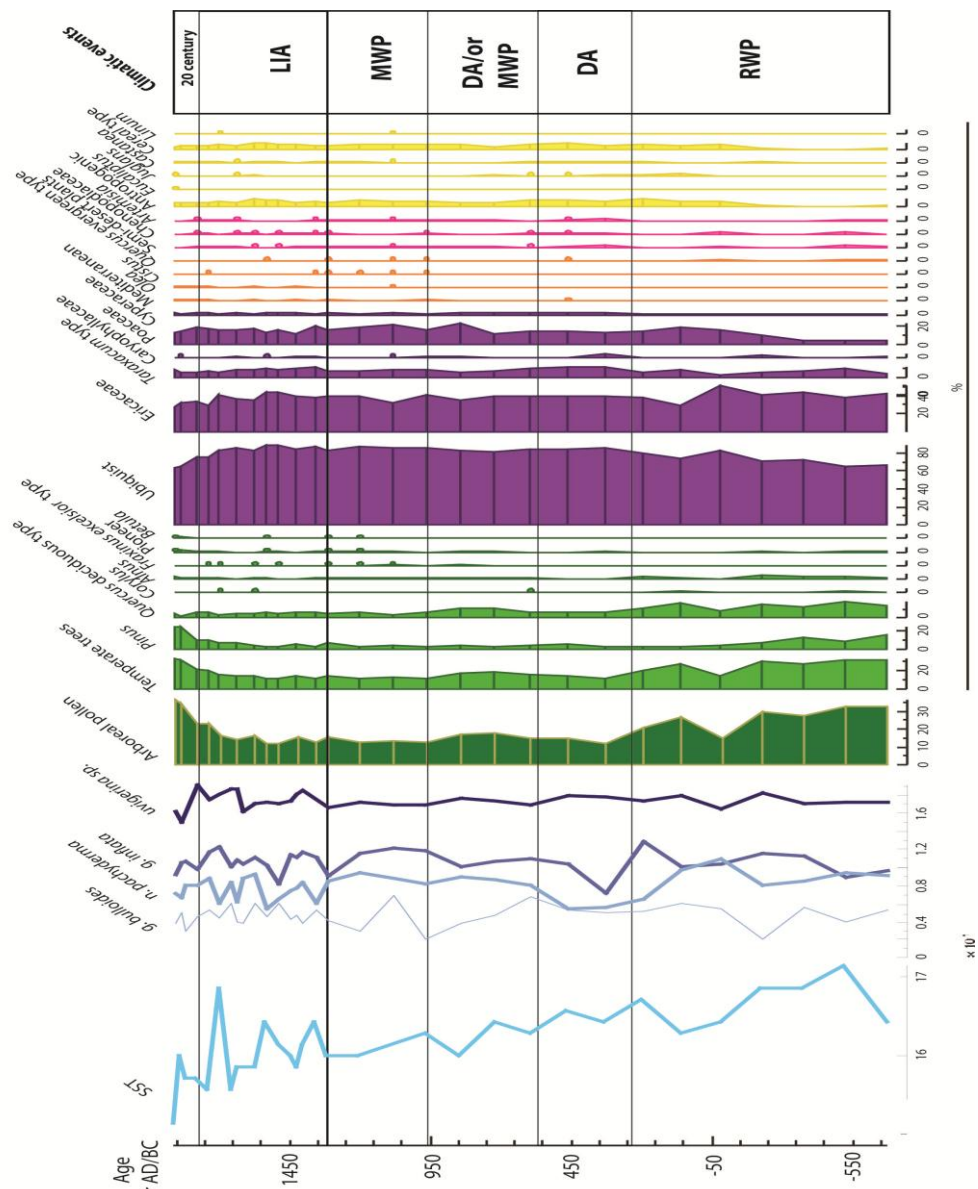


Figure 26 - Vegetation changes, quantitative Sea Surface Temperature (SST) variability and planktonic $\delta^{18}\text{O}$ -isotope composition from DIVA09.

In Figure 27 are presented the variability of terrestrial input proxies (total pollen and spores concentration, alcohols and alkanes) with grain-size parameters (silt and clay) that show a great similarity between them, excepting K/Al ratios and sand. The later suggests the association between potassium feldspar and sand and indicate a grain-size control on all this proxy distribution.

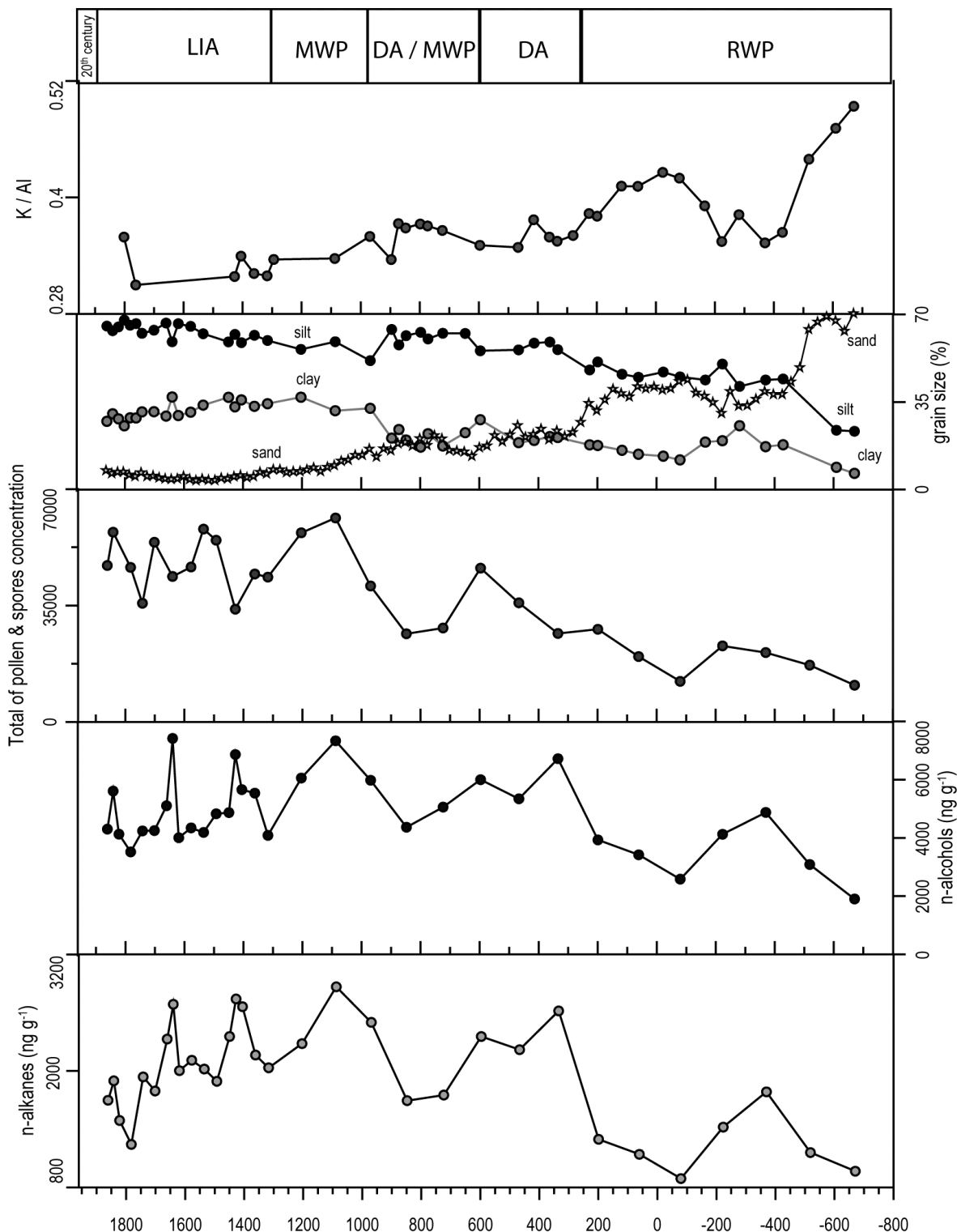


Figure 27 - Comparison between different proxies of terrestrial inputs on DIVA09 and definition of climatic events: LIA (Little Ice Age), MWP (Medieval Warm Period), MWP/DA (Medieval Warm Period/Dark Ages), DA (Dark Ages) and RWP (Roman Warm Period).

The first climatic event, occurring between the core basement (670BC) and 250AD, reflecting warm and relatively wet conditions over the continent and the highest SST values (about 17° C) of the last 2500 years, marked the Roman Warm Period (RWP) in NW Iberian Peninsula and margin. Although there are some important evidences of human activities in the pollen diagram, as testified by the beginning of the Roman agriculture's practices (e.g. the appearance of continuous cereals curve, *Juglans* and *Castanea*), they do not affect the stability of regional forest communities as revealed by the constant presence of temperate trees, which were probably mainly controlled by climate (Figure 26). Nevertheless, the chronology of this warm event does not entirely coincide with the chronology attributed to the RWP by other authors. In the Iberian Peninsula and adjacent margin several limits have been proposed for this event: 0-500AD (Martinez-Cortizas et al., 1999; Diz et al., 2002); 0-550AD (Abrantes et al., 2005b); 0-300AD (Lebreiro et al., 2006), 0-400AD (Eriksson et al., 2006); 50 BC-250AD (Bernárdez et al., 2008); 250BC-400AD (Desprat et al., 2003); 300BC-550AD (Martin-Chivelet et al., 2011). Assuming the date limits for this event, the timing for the DIVA09 core is overestimated (670BC) since we used an independent second order polynomial adjustment on the accepted and well constrained dated levels below 85cm of core depth. Taking into account palynological evidences of human impact in the DIVA09 core and results revealed by Desprat et al. (2003) in the Ría de Vigo record, it is possible to delimitate ca. 200BC as the date for the continuous presence of *Cerealia* in the Iberian Peninsula. Also, it is known that the appearance of *Castanea* in the Iberian Peninsula occurred before the 1st century AD (ca. 150BC) (Desprat et al., 2003; Carrion et al., 2010) as likely the result of Roman culture practices (Rodriguez et al. 1992; Conedera et al., 2004). In the DIVA09 pollen diagram, the first appearance of chestnut was detected at ca. 219BC. Both palynological evidences in this region are in agreement with the chronology proposed for Romans settlement in the Iberian Peninsula (ca.219BC; http://pt.wikipedia.org/wiki/Invasão_romana_da_peninsula_Ibérica).

Thus, the climatic warming, defining the RWP, was characterized by a temperate forest present probably before the Romans settled in the Iberian Peninsula, i.e. before 219BC. We propose the beginning of this climate warming event for 300BC as revealed by stable carbon isotope records obtained in three caves from N Spain by Martin-Chivelet et al. (2011). Additionally, there are some evidences of the increase of near-bottom water speed flow in the south Iceland basin (Bianchi and McCave, 1999), which started some centuries before the 0AD and peaked at around ca. 100AD, being associated with a warming period (most certainly the RWP).

During this event, the water column was well stratified suggesting poor to no upwelling episodes while a gradual increase of continental input is revealed by the increase in pollen concentration, n-

alkanes and n-alcohols in the study area. These evidences are associated with the negative prevailing mode of the North Atlantic Oscillation (NAO-) also recorded in other northern and southern sites as the Ría de Vigo (Diz et al., 2002), the Ría de Muros (Lebreiro et al., 2006), and the Tagus prodelta (Abrantes et al., 2005b; Lebreiro et al., 2006).

The second climatic event is known as the historical Dark Ages (DA). The DA interval has been recognized in both terrestrial and marine environments of the western Iberia between: 400AD-800AD (Eriksson et al., 2006); 400AD-700AD (Lebreiro et al., 2006; Andrade et al., 2011); 450AD-950AD (Desprat et al., 2003); 300AD-600AD (Martin-Chivelet et al., 2011). In our record it occurs between 250AD and 600AD, and is characterized by continental and sea surface cooling as testified by the forest reduction and a gradual sea surface cooling episode. The slight increase in semi-desert plants suggests a relative dryness in the adjacent continent. These cold and relatively dry conditions have also been detected in both Ría de Vigo (Desprat et al., 2003) and Ría de Muros (Andrade et al., 2011) during the DA. However, these cooling and dryer conditions did not perturb agriculture practices that started some centuries before. In the ocean, the water column was less stratified than in the previous climatic event suggesting an increase of upwelling conditions during summer times, as also observed in the Ría de Muros (Lebreiro et al., 2006) and in the Tagus Prodelta (Abrantes et al., 2005b; Lebreiro et al., 2006) in association with prevailing positive NAO mode (NAO+). Although there is a cooling and dry episode and enhanced upwelling regime in the DIVA09 shelf record, there is a continuous increase of terrestrial input. This increase of terrestrial input does not agree with all other records from both northern Rías and southern Tagus Prodelta. This can be probably due to the fact that the Minho shelf is not directly receiving sediments from the Minho River, but from other sources such as the Douro mud patch.

The third climatic event, occurring between 600AD and 950AD, is marked by a relatively continental warming and still oceanic cool conditions as well as stratified water masses. Although climatic conditions were relatively better for agriculture practices there is a decrease in these *taxa* in the pollen diagram. Historical records suggest a decrease in the population between the 4th to the 9th century in Galicia resulting in a decrease of mine exploitations and a reduction of cultivate lands (Valdez and Sanchez 2001), which could be the cause for these changes detected in the pollen diagram. This decrease of cultivate lands are most likely associated with the DA period. However the increase in temperate trees detected in the DIVA09 core were also recorded in the Ría de Vigo and associated with the Medieval Warm Period (MWP), but during 950AD and 1400AD (Desprat et al., 2003). Also, the DIVA09 record show that the water column was well stratified suggesting the almost absence of the upwelling regime in this region during this period. As described for the previous

climatic event the DA were characterized by cold and a relatively dry climate and a vigorous upwelling regime off NW Iberian Peninsula (this study, Desprat et al., 2003; Lebreiro et al., 2006; Andrade et al., 2011). Therefore, both warming and relatively less dry continental conditions and oceanic decrease on the upwelling intensity could probably be more likely associated with the MWP event. Although the upwelling regime was reduced, there are no evidences for the increase of terrestrial input as it should be expected. Once again, the Minho River is probably not the main source for this continental input and other processes are compromising the signal at this site.

The fourth climatic event, occurring between 950AD-1300AD, is marked by a slight decrease of temperate forest and an increase of Mediterranean *taxa* and semi-desert plants. This suggests a replacement of warm and wet conditions by a more Mediterranean climate characterized by warm and dry summers, and cool and wet winters. The Mediterranean climate is generated by the alternating influence of the subtropical high in summer and westerlies during the winter. Thus, during the summer, the subtropical high is expanded to its largest extent and most poleward position, exerting its influence on subtropical west coasts between 30° and 40°N and S latitude. Subsiding air from the subtropical high creates stable atmospheric conditions when coupled with cold ocean currents along these coasts. When the anticyclone moves equatorward in winter, it is replaced by travelling, frontal cyclones with their attendant precipitation. Annual temperature ranges are generally smaller than those found in marine west coast climates. Unfortunately, we cannot compare our data with that of Desprat et al. (2003) since their pollen diagrams do not shown the Mediterranean *taxa* curve.

The water column was stratified and the upwelling regime was still reduced during summer times and there is a substantial continental input, similar to that observed during the MWP in Ría de Muros (Lebreiro et., 2006; Andrade et al., 2011) and in Ría de Vigo (Diz et al., 2002; Alvarez et al., 2005) suggesting moisture conditions in the NW Iberian Peninsula. In contrast, enhanced upwelling regime was detected in SW Iberian margin and associated with the positive prevailing mode of the NAO (NAO+) during the MWP (Abrantes et al., 2005b; Lebreiro et al., 2006). This disparity of moisture/dryness signals between the northwestern/southwestern Iberian margins under prevailing positive NAO mode is also detected in the climate reconstruction performed by Trigo et al. (2004) using several hydrological and climatological observational data sets.

The fifth pollen climatic event, 1300AD-1700AD, is characterized by a similar pollen assemblage of pollen zone 4, but with relatively high percentages of ubiquists and episodes of appearance and disappearance of semi-desert plants and of Mediterranean *taxa*. This suggests some instability of the NW Iberian Peninsula climate with extremely rapid or instantaneous slight climate changes. This complex signal was also observed in both SST and stable isotopic records of the

DIVA09 core. Therefore, within the “long term cooling” of this short climatic episode SST display a complex pattern of increase and decrease temperatures. Also, there is an alternating situation between stratified and non-stratified water column within a prevailing non-stratified situation. This complex climatic signal can be correlated with the well-known Little Ice Age (LIA). Most records from NW Iberia Peninsula and margin show a sea surface and terrestrial cooling, a general continental dryness and enhanced upwelling regime during this period associated with a prevailing NAO+ mode (Diz et al., 2002; Desprat et al., 2003; Alvarez et al., 2005; Lebreiro et al., 2006; Abrantes et al., 2011, Andrade et al., 2011; Martin-Chivelet et al., 2011) while the Tagus Prodelta is characterized by storminess and excess in precipitation and river discharges under the same prevailing NAO+ mode conditions (Abrantes et al., 2005b; Eriksson et al., 2006; Lebreiro et al., 2006) as testified by the present day reconstruction by Trigo et al. (2004).

Finally, the interval between 1700AD-1880AD, is marked by an increase of *Pinus* percentages and therefore by an increase of temperate trees and arboreal pollen associated with human activities. Indeed, it is known that the beginning of *Pinus* expansion in the Iberian Peninsula has started 300 years ago (Queiroz and Mateus, 1994) and that they reach their maximum abundances in the last century as the result of successive afforestation policies (Valdès and Gil Sánchez, 2001). Although there is an increase of *Pinus*, the rest of the pollen record is similar in their general trends to the previous pollen zone. Marine proxy data also shows similarities with the previous climatic phase suggesting that we are still in the LIA period.

Summary and final considerations

A multi-parameter approach using grain-size, geochronological (^{210}Pb and ^{14}C), geochemical (major and trace elements, organic carbon, biomarkers), microfaunal (diatoms and foraminifera) and pollen data were applied on the DIVA09 gravity core collected on the Galicia Mud Patch. Down-core variability of these parameters are probably indicative of the evolution of hydrodynamic conditions (resulting from different oceanographic conditions induced by both climate variability and small sea-level oscillations) in the area through time, instead of a reliable record of the terrestrial input. Despite the influence of hydrodynamic conditions in the preservation of the sediment record, grain-size, pollen, n-alcohols and n-alkanes data suggest a gradual increase of continental input during the Roman Warm Period and the Dark Ages. Potassium to Al, Fe/Al and Ti/Al ratios temporal variability suggesting higher physical weathering during the RWP during which warm and wet conditions prevailed, reflecting an increase level of precipitation that may be responsible by high river discharges and consequently a major efficiency on the transfer of continental materials to the shelf. However, higher

elemental-Al ratios at the bottom core can also be indicative of higher energetic conditions, responsible by removing fine-grained sediment components. Pollen data were grouped into five ecological assemblages indicating different climatic conditions through time and marking very well certain periods of human activities (e.g. Roman settlement, increasing the use of *Pinus*).

Acknowledgments

This work was financially support by the Natura Miño-Minho Project (0234 NATURA MIÑO_MINHO_1_E). We would like to express our gratitude to Bernardino Vilhena, José Vilhena and Silva Lopes (Unidade de Sondagens - Laboratório Nacional de Energia e Geologia) for recovering mechanical drill cores in the Minho estuary and to Guillermo Francés (Universidad de Vigo) for collecting the DIVA09 gravity core. Special thanks for all UGM-LNEG collaborators (Cremilde Monteiro, Daniel Ferreira, Sandra Lemos, Warley Soares and Rúben Borges) that help in laboratorial work. We also thank to Carlos Antunes for Aquamuseu laboratory facilities support (storage and mechanical drill core sections).

References

- Abrantes, F., 1988. Diatoms assemblages as coastal upwelling indicators in surface sediments off Portugal. *Marine Geology*, 85: 15-39.
- Abrantes, F. 2003. A 340,000 year continental climate record from tropical Africa - news from opal phytoliths from the equatorial Atlantic. *Earth and Planetary Science Letters*, 209: 165-179.
- Abrantes, F., Gil, I., Lopes, C., Castro, M., 2005a. Quantitative diatom analyses – a faster cleaning procedure. *Deep sea Research I* 52: 189-98.
- Abrantes, F., Lebreiro, S., Rodrigues, T., Gil, I., Bartels-Jonsdottir, H., Oliveira, P., Kissel, C., Grimalt, J.O., 2005b. Shallow-marine sediment cores record climate variability and earthquake activity off Lisbon (Portugal) for the last 2000 years. *Quaternary Science Reviews* 24: 1123-1149.
- Abrantes, F., Rodrigues, T., Montanari, B., Santos, C., Witt, L., Lopes, C., Voelker, A., 2011. Climate of the last millennium at the southern pole of the North Atlantic Oscillation: an inner-shelf sediment record of flooding and upwelling. *Climate Research*, 48(2-3): 261-280.
- Ackermann, F., 1980. A procedure for correcting the grain-size effect in heavy metal analysis of estuarine and coastal sediments. *Environmental Technology Letters* 1: 518-527.
- Aira Rodriguez, M.J., Saa, P., Lopez, P., 1992. Cambios del paisaje durante el Holoceno: Analisis de polen en Turberas (Galicia, España). *Revue de Paléobiologie* 11: 243-254.
- Andersen, C., Koç, N., Jennings, A., Andrews, J.T., 2004. Nonuniform response of the major surface currents in the Nordic Seas to insolation forcing: Implications for the Holocene climate variability. *Paleoceanography* 19: 1-16.
- Andrade, A., Rubio, B., Rey, D., Álvarez-Iglesias, P., Bernabeu, A.M., Vilas, F., 2011. Palaeoclimatic changes in the NW Iberian Peninsula during the last 3000 years inferred from diagenetic proxies in the Ría de Muros sedimentary record. *Climate Research* 48:247-259.
- Appleby, P., Oldfield, F., 1992. Applications of lead-210 to sedimentation studies. In: Ivanovich, M., Harmon, R.S. (Eds.), *Uranium Series Disequilibrium. Applications to Earth, Marine and Environmental Sciences*. Clarendon Press, Oxford: 731-778 pp.
- Araújo, F., Jouanneau, J.-M., Valério, P., Barbosa, T., Gouveia, A., Weber, O., Oliveira, A., Rodrigues, A., Dias, J., 2002. Geochemical tracers of northern Portuguese estuarine sediments on the shelf. *Progress in Oceanography* 52: 277-297.
- Araújo, M., Dias, J., Jouanneau, J.-M., 1994. Chemical characterisation of the main fine sedimentary deposit at the northwestern Portuguese shelf. *GAIA* 9: 59-65.
- Bard, E., Rostek, F., Menot-Combes, G., 2004. Radiocarbon calibration beyond 20.000 ¹⁴C yr B.P. by means of planktonic foraminifera of the Iberian Margin. *Quaternary Research* 61: 204-214.
- Battarbee, R.W., 1973. A new method for estimation of absolute microfossil numbers with reference especially to diatoms. *Limnology and Oceanography* 18: 647-652.

-
- Berger, A., 1978. Long-term variations of calorific insolation resulting from the earth's orbital elements. *Quaternary Research* 9: 139-167.
- Bernárdez, P., González-Álvarez, R., Francés, G., Prego, R., Bárcena, M.A., Romero, O.E., 2008. Palaeoproductivity changes and upwelling variability in the Galicia Mud Patch during the last 5000 years: geochemical and microfloral evidence. *Holocene* 18: 1207-1218
- Bettencourt, A., Ramos, L. (Eds.), 2003. *Estuários Portugueses*. Instituto da Água, Lisboa.
- Bianchi, G. G., Mccave, I. N., 1999. Holocene Periodicity in North Atlantic Climate and Deep-Ocean Flow South of Iceland. *Nature* 397: 515-17.
- Boer, W., van den Bergh, G.D., de Haas, H., de Stigter, H.C., Gieles, R., van Weering, T.C.E., 2006. Validation of accumulation rates in Teluk Banten (Indonesia) from commonly applied ²¹⁰Pb models, using the 1883 Krakatau tephra as time marker. *Marine Geology* 227: 263-277.
- Bottema, S., van Straaten, L.M.J.U., 1966. Malacology and palynology of two cores from the Adriatic sea floor. *Marine Geology* 4: 553-564.
- Braun-Blanquet, J., Pinto da Silva, A.R., Rozeira, A., 1956. Résultats de deux excursions géobotaniques à travers le Portugal septentrional et moyen. II. Chenaies à feuilles caduques (*Quercion occidentale*) et chenaies à feuilles persistentes (*Quercion faginea*) au Portugal. *Agronomia Lusitana* 18: 167-234.
- Cato, I., 1977. Recent sedimentological and geochemical conditions and pollution problems in two marine areas in Soutwestern Sweden. *Striae* 6: 150 pp.
- Carrión, J.S., Sánchez-Gómez, P., 1992. Palynological data in support of the survival of Walnut (*Juglans regia* L.) in the western Mediterranean area during last glacial times. *Journal of Biogeography* 19: 623-630.
- Carrión, J.S., Fernández, S., Jiménez-Moreno, G., Fauquette, S., Gil-Romera, G., González-Sampérez, P., Finlayson C., 2010. The historical origins of aridity and vegetation degradation in southeastern Spain. *Journal of Arid Environments* 74: 731-736.
- Conedera, M., Krebs, P., Tinner, W., Pradella, M., Torroni, D., 2004. The cultivation of *Castanea sativa* (Mill.) in Europe: from its origin to its diffusion on a continental scale. *Vegetation and Archaeobotany* 13: 161-179.
- Costa, A.M., Mil-Homens, M., Lebreiro, S.M., Richter, T.O., de Stigter, H., Boer, W., Trancoso, M.A., Melo, Z., Mouro, F., Mateus, M., Canário, J., Branco, V., Caetano, M., 2011. Origin and transport of trace metals deposited in the canyons off Lisboa and adjacent slopes (Portuguese Margin) in the last century. *Marine Geology* 282: 169-177.
- Crucifix, M., Loutre, M.F., Tulkens, P., Fichetef, T., Berger, A., 2002. Climate evolution during the Holocene: a study with an Earth system model of intermediate complexity. *Climate Dynamics* 19: 43-60.
- de Stigter, H.C., Boer, W., de Jesus Mendes, P.A., Jesus, C.C., Thomsen, L., van den Bergh, G.D., van Weering, T.C.E., 2007. Recent sediment transport and deposition in the Nazare Canyon, Portuguese continental margin. *Marine Geology* 246: 144-164.
- de Vernal, A., Henry, M., Bilodeau, G., 1996. Techniques de préparation et d'analyse en micropaléontologie. Les cahiers du GEOTOP. Département des Sciences de la terre. Québec University, Montréal 3: 16-27.
- Desprat, S., Sánchez-Goñi, M.F., Loutre, M.F., 2003. Revealing climatic variability of the last three millennia in northwestern Iberia using pollen influx data. *Earth and Planetary Science Letters* 213: 63-78.
- Desprat, S., 2005. Réponses climatiques marines et continentales du SW de L'Europe lors des derniers interglaciaires et des entrée en glaciation. PhD Thesis, Bordeaux 1 University, Bordeaux (France): 282 pp.
- Dias, J., 1987. Dinâmica sedimentar e evolução recente da plataforma continental Portuguesa setentrional. PhD Thesis, Faculdade de Ciências da Universidade de Lisboa: 384 pp.
- Dias, J., Gonzalez, R., Garcia, C., Dias-del-Rio, V., 2002a. Sediment distribution patterns on the Galicia-Minho continental shelf. *Progress in Oceanography* 52: 215-231.
- Dias, J., Jouanneau, J.-M., Gonzalez, R., Araújo, F., Drago, T., Garcia, C., Oliveira, A., Rodrigues, A., Vitorino, F., Weber, O., 2002b. Present day sedimentary processes in the northern Iberian shelf. *Progress in Oceanography* 52: 249-259.
- Drago, T., Oliveira, A., Dias, J., Magalhães, F., Cascalho, J., Jouanneau, J.-M., Vitorino, J., 1998. Some evidences of northward fine sediment transport in the northern Portuguese continental shelf. *Oceanologica Acta* 21: 223-231.
- Diz, P., Francés, G., Pelejero, C., Grimalt, J.O., Vilas, F., 2002. The last 3000 years in the Ría de Vigo (NW Iberian Margin): climatic and hydrographic signals. *Holocene* 12: 459-468.
- Eglinton, G., Hamilton, R.J., 1967. Leaf epicuticular waxes. *Science* 156: 1322-1335.
- Grimalt, J.O., Calvo, E., Pelejero, C., 2001. Sea Surface pleotemperature errors in Uk'37 estimation due to alkenone measurements near the limit of detection. *Paleoceanography* 16: 226-232.
- Groot, J.J., Groot, C.R., 1966. Pollen spectra from deep-sea sediments as indicators of climatic changes in southern South America. *Marine Geology* 4: 525-537.
- Heusser, L.E., Balsam, W.L., 1977. Pollen distribution in the N.E. Pacific Ocean. *Quaternary Research* 7: 45-62.
- Heusser, L.E., Stock, C.E., 1984. Preparation techniques for concentrating pollen from marine sediments and other sediments with low pollen density. *Palynology* 8: 225-227.
- Hughen, K.A., Baillie, M.G.L., Bard, E., Bayliss, A., Beck, J.W., Bertrand, C., Blackwell, P.G., Buck, C.E., Burr, G., Cutler, K.B., Damon, P.E., Edwards, R.L., Fairbanks, R.G., Friedrich, M., Guilderson, T.P., Kromer, B., McCormac, F.G., Manning, S., Bronk Ramsey, C., Reimer, P.J., Reimer, R.W., Remmele, S., Southon, J.R., Stuiver, M., Talamo, S., Taylor,
-

F.W., van der Plicht, J., Weyhenmeyer, C.E., 2004. Marine 04 Marine Radiocarbon Age Calibration, 0-26 Cal kyr BP. *Radiocarbon* 46: 1059-1086.

Jansen, J.H.F., Alderliesten, C., Houston, C.M. et al. 1989. Aridity in equatorial Africa during the last 225,000 years: a record of opal phytoliths/freshwater diatoms from the Zaire (Congo) deep-sea fan (northeast Angola basin), *Radiocarbon* 31:557-569.

Johnsen, S.J., Dahl-Jensen, D., Gundestrup, N., Steffensen, J.P., Clausen, H.B., Miller, H., Masson-Delmotte, V., Sveinbjörnsdóttir, A.E., White, J., 2001. Oxygen isotope and palaeotemperature records from six Greenland ice-core stations: Camp Century, Dye-3, GRIP, GISP2, Renland and NorthGRIP. *Journal of Quaternary Science* 16, 299-307

Jouanneau, J.-M., Weber, O., Drago, T., Rodrigues, A., Oliveira, A., Dias, J., Garcia, C., Schmidt, S., Reyss, J., 2002. Recent sedimentation and sedimentary budgets on the western Iberian shelf. *Progress in Oceanography* 52: 261-275.

Koreneva, E.V., 1966. Marine palynological researches in the U.R.S.S.. *Marine Geology* 4: 565-574.

Kutzbach, J.E. and Gallimore, R.G. (1988). Sensitivity of a coupled atmosphere/mixed layer ocean model to changes in orbital forcing at 9000 years B.P.. *Journal of Geophysical Research* 93: 803-821.

Lantzsch, H., Hanebuth, T.J.J., Bender, V.B., 2009a. Holocene evolution of mud depocentres on a high-energy, low-accumulation shelf (NW Iberia). *Quaternary Research* 72: 325-336.

Lantzsch, H., Hanebuth, T.J.J., Bender, V.B., Krastel, S., 2009b. Sedimentary architecture of a low-accumulation shelf since the Late Pleistocene (NW Iberia). *Marine Geology* 259: 47-58.

Lantzsch, H., Hanebuth, T.J.J., Henrich, R., 2010. Sediment recycling and adjustment of deposition during deglacial drowning of a low-accumulation shelf (NW Iberia). *Continental Shelf Research* 30: 1665-1679.

Loring, D., 1990. Lithium - A new approach for the granulometric normalization of trace metal data. *Marine Chemistry* 29: 155-168.

Loureiro, J., Machado, M., Macedo, M., Nunes, M., Botelho, O., Sousa, M., Almeida, M., Martins, J., 1986. *Monografias hidrológicas dos principais cursos de água de Portugal continental*. Direcção-Geral dos Recursos e Aproveitamentos Hidráulicos, Lisboa, 569 pp.

Lorenz, S. J., Kim, J.-H., Rimbu, N., Schneider, R.R., Lohmann, G., 2006. Orbitally driven insolation forcing on Holocene climate trends: Evidence from alkenone data and climate modeling. *Paleoceanography* 21: 1-14.

Magri, D., 1995. Some questions on the Late-Holocene vegetation of Europe. *The Holocene* 5: 354-360.

Marlowe, I.T., Brassell, S.C., Eglinton, G., Green, J.C., 1984. Long chain unsaturated Ketones and esters in living algae and marine sediments. *Org. Geochemistry* 6: 135-141.

Marshall, J., Jones, H., Karsten, R., Wardle, R., 2002. Can eddies set ocean stratification? *Journal of Physical Oceanography* 32: 26-39.

Martín-Chivelet, J., Muñoz-García, M.B., Edwards, R.L., Turrero, M.J., Ortega, A.I., 2011. Land surface temperature changes in Northern Iberia since 4000 yr BP, based on $d^{13}C$ of speleothems. *Global and Planetary Change* 77: 1-12.

Martínez-Cortizas, A., Pontevedra-Pombal, X., García-Rodeja, E., Nóvoa-Muñoz, J.C., Shotyk, W., 1999. Mercury in a Spanish peat bog: archive of climate change and atmospheric metal deposition. *Science* 284: 939-942.

Martins, V., Jouanneau, J.-M., Weber, O., Rocha, F., 2006. Tracing the late Holocene evolution of the NW Iberian upwelling system. *Marine micropaleontology* 59: 35-55.

McCave, I.N., Hall, I.R., 2002. Turbidity of waters over the Northwest Iberian continental margin. *Progress in Oceanography* 52: 299-313.

Meyers, P., 1994. Preservation of elemental and isotopic source identification of sedimentary organic matter. *Chemical Geology* 114: 289-302.

Meyers, P., 1997. Organic geochemical proxies of paleoceanographic, paleolimnologic, and paleoclimatic processes. *Organic Geochemistry* 27: 213-250.

Moros, M., Emeis, K., Risebrobakken, B., Snowball, I., Kuijpers, A., McManus, J., Jansen, E., 2004. Sea surface temperatures and ice rafting in the Holocene North Atlantic: climate influences on northern Europe and Greenland. *Quaternary Science Reviews* 23, 2113-2126.

Muler, P., Kirst, G., Ruhland, G., Storch, I.v., Rosell-Melé, A., 1998. Calibration of the alkenone index Uk'37 based on core-tops the eastern South Atlantic and global ocean (60°N-60°S). *Geochimica et Cosmochimica Acta* 62: 1757-1772.

Muller, J., 1959. Palynology of recent Orinoco delta and shelf sediments. *Micropaleontology* 5: 1-32.

Nriagu, J.O., 1996. A history of global metal pollution. *Science* 272: 223.

Oliveira, A., Rocha, F., Rodrigues, A., Jouanneau, J.-M., Dias, J., Weber, O., Gomes, C., 2002a. Clay minerals from the sedimentary cover from the Northwest Iberian shelf. *Progress in Oceanography* 52: 233-247.

Oliveira, A., Vitorino, J., Rodrigues, A., Jouanneau, J.-M., Dias, J., Weber, O., 2002b. Nepheloid layer dynamics in the northern Portuguese shelf. *Progress in Oceanography* 52: 195-213.

Patterson, C.C., 1972. Silver stocks and losses in ancient and Medieval times. *The Economic History Review* 25 (Second Series): 205-235.

Polunin, O., Walters, M., 1985. *A guide to the vegetation of Britain and Europe*. Oxford University Press, New York: 238 pp.

-
- Pons A., Reille, M., 1986. Nouvelles recherches pollenanalytiques à Padul (Granada) : La fin du dernier glaciaire et l'Holocène. E. López-Vera (Ed.). Quaternary climate in Western Mediterranean, University Autónoma de Madrid, 405-420.
- Poppe, L.J., Eliason, A.H., 2008. A Visual Basic program to plot sediment grain-size data on ternary diagrams. *Computers & Geosciences* 34: 561-565.
- Prahl, F., Wakeham, S.G., 1987. Calibration of unsaturation patterns in long-chain ketones compositions for palaeotemperature assessment. *Nature* 330: 367-369.
- Queiroz, P.F., Mateus, J.E., 1994. Preliminary palynological studies at Lagoa de Albufeira and Lagoa de Melides, Portugal. *Revista de Biologia* 15, 1527.
- Reimer, P.J., Baillie, M.G.L., Bard, E., Bayliss, A., Beck, J.W., Blackwell, P.G., Buck, C.E., Burr, G.S., Cutler, K.B., Damon, P.E., Edwards, R.L., Fairbanks, R.G., Friedrich, M., Guilderson, T.P., Hughen, K.A., Kromer, B., McCormac, F.G., Manning, S.W., Ramsey, C.B., Reimer, R.W., Remmele, S., Southon, J.R., Stuiver, M., Talamo, S., Taylor, F.W., van der Plicht, J., and Weyhenmeyer, C.E. 2004. IntCal04 Terrestrial radiocarbon age calibration, 0-26 cal kyr BP. *Radiocarbon* 46: 1029-1058.
- Renssen, H., Goosse, H., Fichefet, T., Brovkin, V., Driesschaert, E., Wolk, F., 2005. Simulating the Holocene climate evolution at northern high latitudes using a coupled atmosphere-sea ice-ocean-vegetation model. *Climate Dynamics* 24: 23-43.
- Rodrigues, T., Grimalt, J.O., Abrantes, F.G., Flores, J.A., Lebreiro, S.M., 2009. Holocene interdependences of changes in sea surface temperature, productivity, and fluvial inputs in the Iberian continental shelf (Tagus mud patch). *Geochemistry, Geophysics Geosystems* 10: Q07U06.
- Salgueiro, E., Voelker, A., Abrantes, F., Meggers, H., Pflaumann, U., Lončarić, N., González-Álvarez, R., Oliveira, P., Bartels-Jónsdóttir, H.B., Moreno, J., Wefer, G., 2008. Planktonic foraminifera from modern sediments reflect upwelling patterns off Iberia: Insights from a regional transfer function. *Marine Micropaleontology* 66: 135-164.
- Schiff, K., Weisberg, S., 1999. Iron as a reference element for determining trace metal enrichment in Southern California coastal shelf sediments. *Marine Environmental Research* 48: 161-176.
- Schneider, R. R., Price, B., Müller, P. J., Kroon, D., Alexander, I. 1997. Monsoon related variations in Zaire (Congo) sediment load and influence of fluvial silicate supply on marine productivity in the east equatorial Atlantic during the last 200,000 years. *Paleoceanography* 12: 463-481.
- Schrader, H.J., Gersonde, R. 1978. Diatoms and silicoflagellates. *Utrecht Micropaleontology Bulletin* 17: 125-132.
- Schubert, C., Calvert, S., 2001. Nitrogen and carbon isotopic composition of marine and terrestrial organic matter in Arctic Ocean sediments: Implications for nutrient utilization and organic matter composition. *Deep Sea Research Part I: Oceanographic Research Papers* 48: 789-810.
- Shepard, F., 1954. Nomenclature based on sand-silt-clay ratios, *Journal of Sedimentary Petrology*: 151-158.
- Sousa, R., Guilhermino, L., Antunes, C., 2005. Molluscan fauna in the freshwater tidal area of the River Minho estuary, NW of Iberian Peninsula. *Annales de Limnologie - International Journal of Limnology* 41: 141-147.
- Stein, R., Rack, F., 1995. A 160,000 year high-resolution record of quantity and composition of organic carbon in the Santa Barbara Basin (site 893). In: Kennett, J., Baldauf, J., Lyle, M. (Eds.), *Proceedings of Ocean Drilling Program*: 125-138.
- Stuiver, M., Reimer, P.J., 1993. Extended ^{14}C database and revised CALIB radiocarbon calibration program. *Radiocarbon* 35: 215-230.
- Stuiver, M., Reimer, P.J., Reimer, R.W., 2005. CALIB 5.0.
- Telford, R.J., Heegaard, E., Birks, H.J.B., 2004. The intercept is a poor estimate of a calibrated radiocarbon age. *The Holocene* 14: 296-298.
- Trigo, R., Pozo-Vazquez, D., Osborn, T., Castro-Diez, Y., Gamis-Fortis, S., Esteban-Parra, M., 2004. North Atlantic oscillation influence on precipitation, river flow and water resources in the Iberian Peninsula. *International Journal of Climatology* 24:925-944
- Turon, J.-L., 1984. Le palynoplancton dans l'environnement actuel de l'Atlantique nord-oriental. Evolution climatique et hydrologique depuis le dernier maximum glaciaire. Mémoires de l'Institut de Géologie du bassin d'Aquitaine, 17. Université de Bordeaux I, Bordeaux, 313 pp.
- Valdès, C.M., Gil Sanchez, L., 2001. La transformación histórica del paisaje forestal en Galicia, Ministerio de Medio Ambiente, 159 pp..
- Valette-Silver, N., 1993. The use of sediment cores to reconstruct historical trends in contamination of estuarine and coastal sediments. *Estuaries* 16: 577-588.
- van der Kaars, S., de Deckker, P., 2003. Pollen distribution in marine surface sediments offshore Western Australia. *Reviews in Palaeobotany and Palynology* 124: 113-129.
- van Weering, T., de Stigter, H., Boer, W., de Haas, H., 2002. Recent sediment transport and accumulation on the NW Iberian margin. *Progress in Oceanography* 52: 349-371.
- Villanueva, J., 1996. Estudi de les variacions climàtiques i oceanogràfiques a l'atlàntic Nord Durant els últims 300.000 anys mitjançant l'anàlisi de marcadors moleculars., Ramon Llull, Barcelona, 186 pp.
-

-
- Villanueva, J., Calvo, E., C.Pelejero, Grimalt, J.O., Boelaert, A., Labeyrie, L., 2001. A latitudinal productivity band in the central North Atlantic over the last 270 Kyr: An alkenone perspective. *Paleoceanography* 16: 1-10.
- Volkman, J.K., Eglinton, G., Corner, E.D.S., Forsberg, T.E.V., 1980. Long-chain Alkenes and Alkenones in the Marine Coccolithophorid *Emiliania Huxleyi*. *Phytochemistry* 19: 2619-2622.
- Weber, S.L., Oerlemans, J., 2003. Holocene glacier variability: three case studies using an intermediate-complexity climate model. *The Holocene* 13, 353-363.
- Windom, H., Schropp, S., Calder, F., Ryan, J., Smith, R., Burney, L., Lewis, F., Rawlinson, C., 1989. Natural trace metal concentrations in estuarine and coastal marine sediments of the southeastern United States. *Environmental Science and Technology* 23: 314-320.
- Yarincik, K.M., Murray, R.W., Peterson, L.C., 2000. Climatically Sensitive Eolian and Hemipelagic Deposition in the Cariaco Basin, Venezuela, Over the Past 578,000 Years: Results From Al/Ti and K/Al. *Paleoceanography* 15: 210-228.
- Zabel, M., Bickert, T., Dittert, L., Haese, R.R., 1999. Significance of the Sedimentary Al : Ti Ratio as an Indicator for Variations in the Circulation Patterns of the Equatorial North Atlantic. *Paleoceanography* 14: 789-799.
- Zabel, M., Schneider, R.R., Wagner, T., Adegbe, A.T., de Vries, U., Kolonic, S., 2001. Late Quaternary Climate Changes in Central Africa as Inferred from Terrigenous Input to the Niger Fan. *Quaternary Research* 56: 207-217.